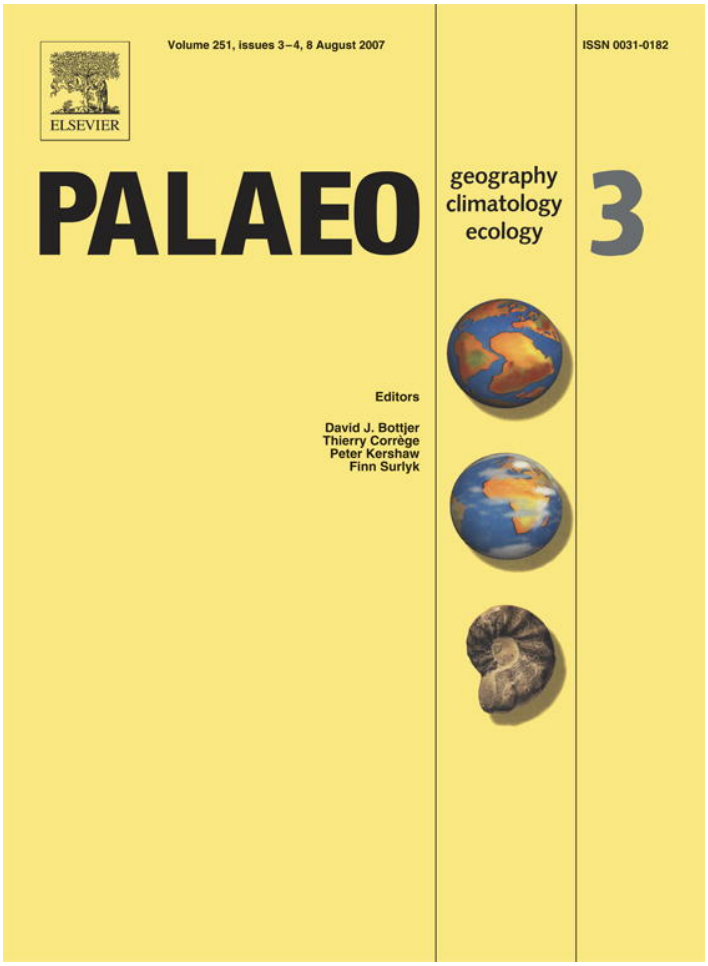

Available online at www.sciencedirect.com
ScienceDirect
ELSEVIER
Palaeogeography, Palaeoclimatology, Palaeoecology 251 (2007) 527–546
PALAEO
www.elsevier.com/locate/palaeo

Palaeoceanographic and palaeoclimatic reorganization around the Middle–Late Jurassic transition

Pauline Rais *, Beat Louis-Schmid, Stefano M. Bernasconi, Helmut Weissert

Geological Institute, ETH-Zurich, 8092 Zurich, Switzerland

Received 30 January 2006; received in revised form 4 May 2007; accepted 8 May 2007

Abstract

A Middle to Upper Jurassic succession of submarine hardgrounds overlain by nodular limestones is exposed in the Jura mountains and in the Helvetic of the Swiss Alps. These sediments were accumulated along the northern shelf of the east–west trending Tethys seaway. Submarine hardgrounds and nodular limestones were also formed on the Briançonnais High, today outcropping in the middle Penninic nappe pile of the Alps. Hardgrounds record strong and persistent current activity along the northern Tethys shelf and on the Briançonnais High during the Callovian and Early Oxfordian. The transition from hardgrounds to nodular limestones corresponds to a major reorganization of Tethys oceanography. The change occurred in Plicatilis ammonite Zone (Middle Oxfordian). Carbon isotope stratigraphy, calibrated against an ammonite-dated reference section in the French Subalpine Basin, serves as a correlation tool between ammonite-dated sections and successions with poor biostratigraphic resolution. Correlation demonstrates that the end of hardground formation was synchronous over wide parts of the northern Tethys. The change in shelf sedimentation coincides with a positive carbon isotope excursion with an amplitude of 1.5‰. The change in C-isotope stratigraphy indicates that observed reorganization of current patterns along the northern Tethys shelf was coupled with global change in oceanography and climate. We propose that the change in northern Tethys sedimentation was caused by opening of new seaways at a time of progressive collapse of Pangaea.

Keywords: Palaeoceanography; Tethys; Oxfordian; Hardgrounds; Chemostratigraphy; Palaeocirculation

1. Introduction

Middle to Late Jurassic sediments presently outcropping in the Jura mountains and in the Helvetic and Penninic nappe pile of the Alps provide an archive of significant changes in oceanography and climate (Sandy, 1991; Norris and Hallam, 1995; Jenkyns, 1996; Pellenard et al., 1999; Abbink et al., 2001; Dromart et al., 2003a,b). Submarine hardgrounds formed during the Callovian and Early Oxfordian over wide areas of the northern Tethys shelf and on the Briançonnais High (Furrer, 1979; Norris and Hallam, 1995; Collin et al., 2005). Low sediment accumulation rates on outer-shelf to upper slope environments coincided with the deposition of organic-carbon enriched hemipelagic marlstones in basins along the northern Tethys and with radiolarites in deep pelagic settings (Baumgartner, 1987; Tribovillard, 1988; Norris and Hallam, 1995; Dromart et al., 2003a). A change in the sedimentation pattern occurred in the Middle Oxfordian. Carbonate sedimentation became dominant over wide parts of the northern Tethys, with the development of new

* Corresponding author. Fax: +41 446321075.
E-mail address: pauline.rais@alumni.ethz.ch (P. Rais).

0031-0182/$ - see front matter © 2007 Elsevier B.V. All rights reserved.
doi:10.1016/j.palaeo.2007.05.008

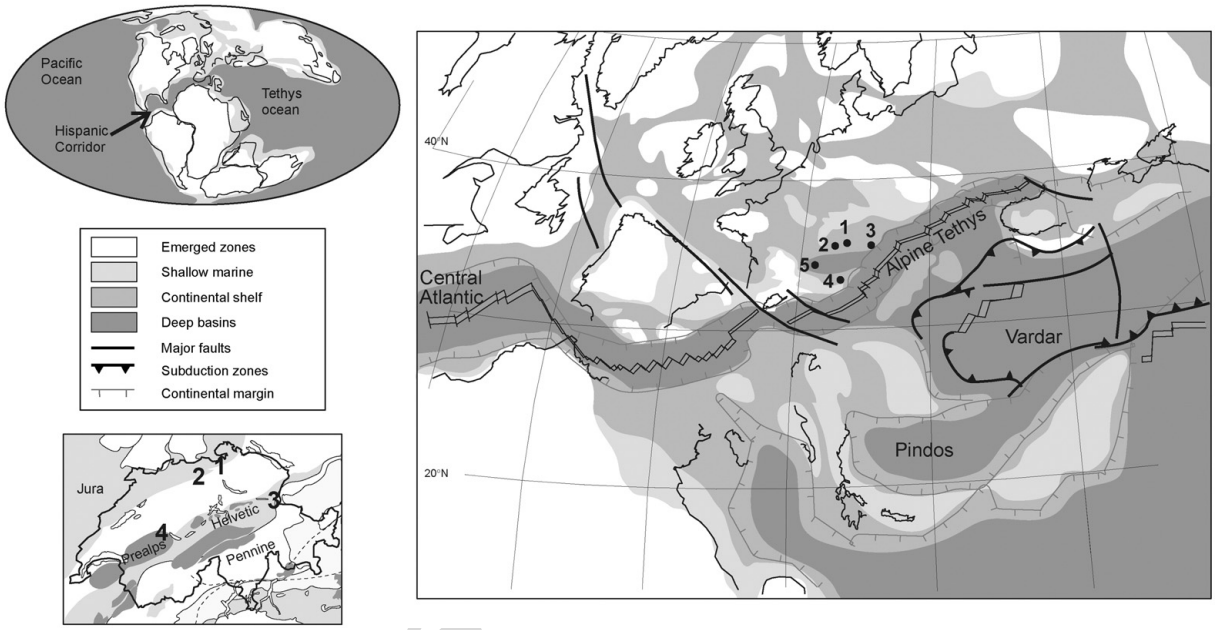

Fig. 1. Position of the sections on palaeogeographic and tectonic maps. 1: Weiach; 2: Auenstein; 3: Nissibach; 4: Gantrisch; 5: Subalpine Basin. World map of the Late Jurassic, modified after Scotese (2001). Western Tethys map of the Oxfordian, compiled and modified after Stampfli and Borel (2002) (for tectonic and continent position), Ziegler (1988) and Thierry et al. (2000a,b) (for depositional environments).

reef sites and the expansion of calcareous nannofossils (Bartolini et al., 1996; Leinfelder et al., 2002; Cecca et al., 2005).

The observed change in Tethys sedimentation occurred at a time of progressive fragmentation of Pangaea (Dercourt et al., 1994). New oceanic gateways were formed with, in particular, the opening of the Hispanic Corridor, connecting the Pacific to the western Tethys Ocean (Ziegler, 1988; Scotese, 2001). Ocean floor spreading rates were especially high during the Callovian and the Oxfordian (Jones et al., 1994; Corbin et al., 2000; Cogne and Humler, 2004).

The Callovian–Oxfordian is also marked by a significant temperature increase which is well documented at high latitudes (Riboulleau et al., 1998). Oxygen isotope composition of belemnites from the Russian platform, sporomorph data from the North Sea (Abbink et al., 2001) and the migration of Tethyan ammonites to higher latitudes (Enay, 1980) all provide evidence for substantial warming during the Oxfordian. The temperature increase was accompanied by an extension of the arid climate belt in the northern hemisphere documented by studies on palynology and clay mineralogy, and by the distribution of evaporites and coal (Hallam, 1985; Rioult et al., 1991; Abbink et al., 2001; Hautevelle, 2005).

For this study we traced the Callovian–Oxfordian evolution of the Tethys Ocean in sedimentary archives from the northern Tethys. The northern Tethyan margin is an appropriate area to investigate palaeoceanographic changes, as it is situated along a sensible west–east trending seaway connecting the opening Atlantic Ocean with the eastern Tethys. Biostratigraphy and carbon-isotope stratigraphy were used as a correlation tool to establish a chronology of oceanic changes in the northwestern Tethys. We propose that observed changes in Tethys sedimentation were triggered by a reorganization of Tethys–Atlantic oceanography triggered by the opening and deepening of the Hispanic corridor (Dercourt et al., 1994).

2. Study sites

In this study we investigated four sections situated in Switzerland. The section "Weiach", a drill hole section, is situated north of Zurich. The Auenstein section is located in the Jura mountains of Northern Switzerland. The Nissibach section in northeastern Switzerland geologically belongs to the Helvetic nappe pile. The middle Penninic Gantrisch section is located in the Prealps in western Switzerland (Fig. 1). The studied sediments were deposited on the northern continental shelf of the Alpine Tethys at palaeolatitudes of approximately 35°N (Smith et al., 1994; Stampfli and Borel, 2002) (Fig. 1). The chosen localities provide a good overall picture of the depositional environment prevailing along the northern Tethyan shelf during the Callovian–Oxfordian.

2.1. Weiach

The Weiach section (Fig. 2) is from a borehole situated near the village of Glattfelden that was drilled in 1983 by the NAGRA (Swiss National Cooperative for the Storage of Radioactive Waste). The Middle–Upper Jurassic sediments were formed in a shelf-trough of up to a few hundred meters depth influenced by detrital input (Allenbach, 2001). The sediments consist predominantly of limestone and claystone, and contain some detrital quartz (Matter et al., 1988). The fauna is mainly pelagic, dominated by cephalopods and thin-shelled bivalves. Biostratigraphic control was obtained by lithological correlation with biostratigraphically dated sections and by the ammonites found within the core (Matter et al., 1988). The Middle Callovian is not represented in the core, reflecting a stratigraphic gap. The Upper Callovian Anceps–Athleta Beds consist of a 1.6 m-thick unit characterized by the presence of incrusted ammonites and belemnites and the abundance of polynucleus iron ooids. The Anceps–Athleta Beds are overlain by 70 cm of Lower Oxfordian glauconitic marls followed by the Birmensdorf Member. We identified the Birmensdorf Member as a 2.8 m thick bed that consists of marlstones with small carbonate lenses and bioclasts. The studied part of the core ends within the lower part of the Effinger Member, a limestone–marl alternation containing belemnites and ammonites.

2.2. Auenstein

The section is exposed in a quarry near the village of Auenstein (Aargau) (Fig. 3). The sediments were deposited on a open-marine shelf, at an estimated depth of approximately 100 m (Gygi and Persoz, 1986). The large amount of bioclasts and the detrital quartz testify the proximity of a platform and of emerged land (Allenbach, 2001). Ammonite stratigraphy indicates very low sedimentation rates and only intermittent sedimentation from the Middle Bathonian to the Late Callovian (Gygi and Marchand, 1982). The Early Oxfordian is represented by the 50 cm-thick Schellenbrücke Bed, which consists of an iron-impregnated limestone bed containing iron ooids and numerous fossils, and topped by a hardground (Gygi and Persoz, 1986). More than 80% of the fauna consists of cephalopods, other fossils consisting of echinoderms,

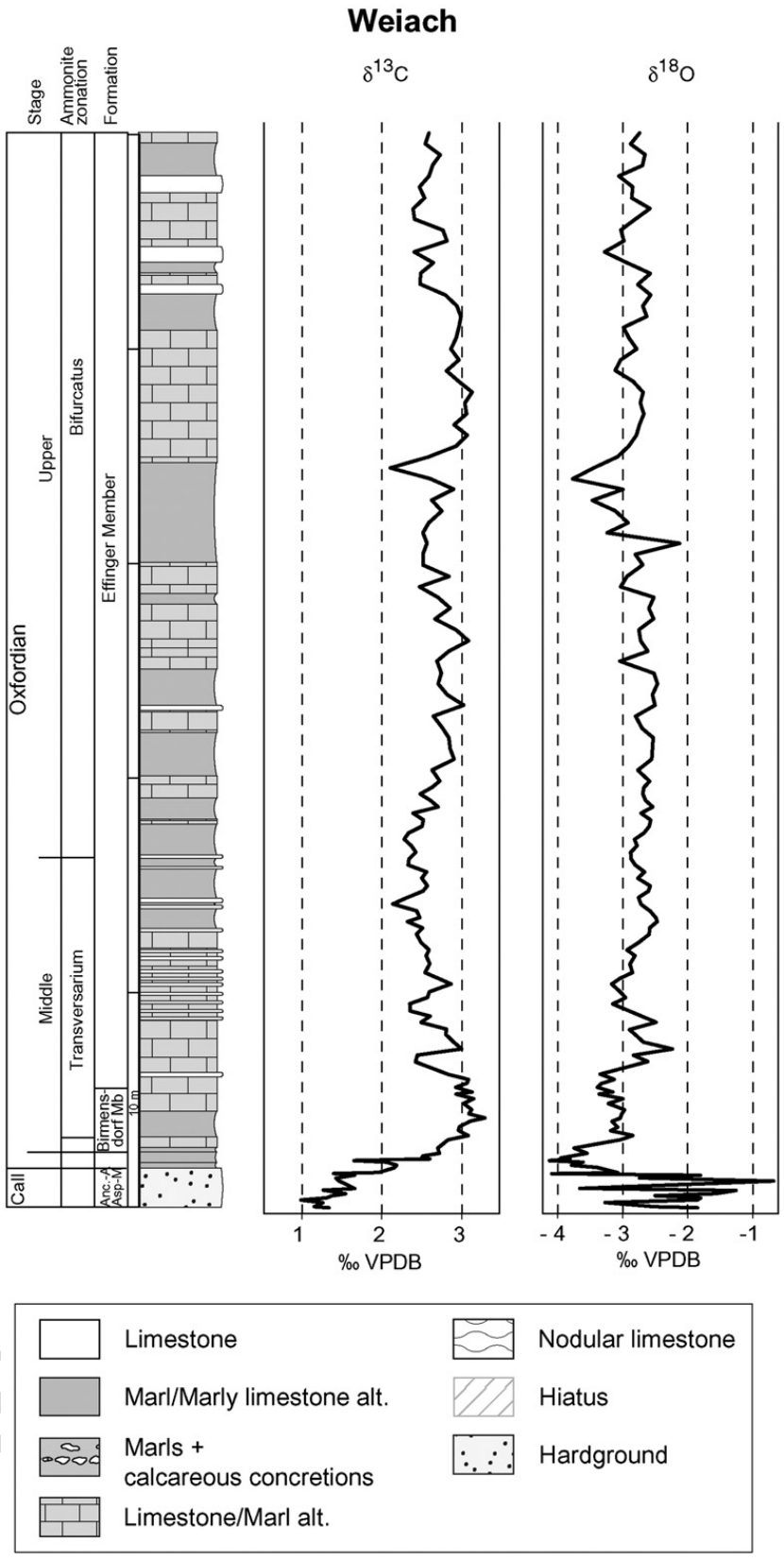

Fig. 2. Lithology, stratigraphy and carbon and oxygen stable isotopes of the Weiach section. Biostratigraphy based on Matter et al. (1988).

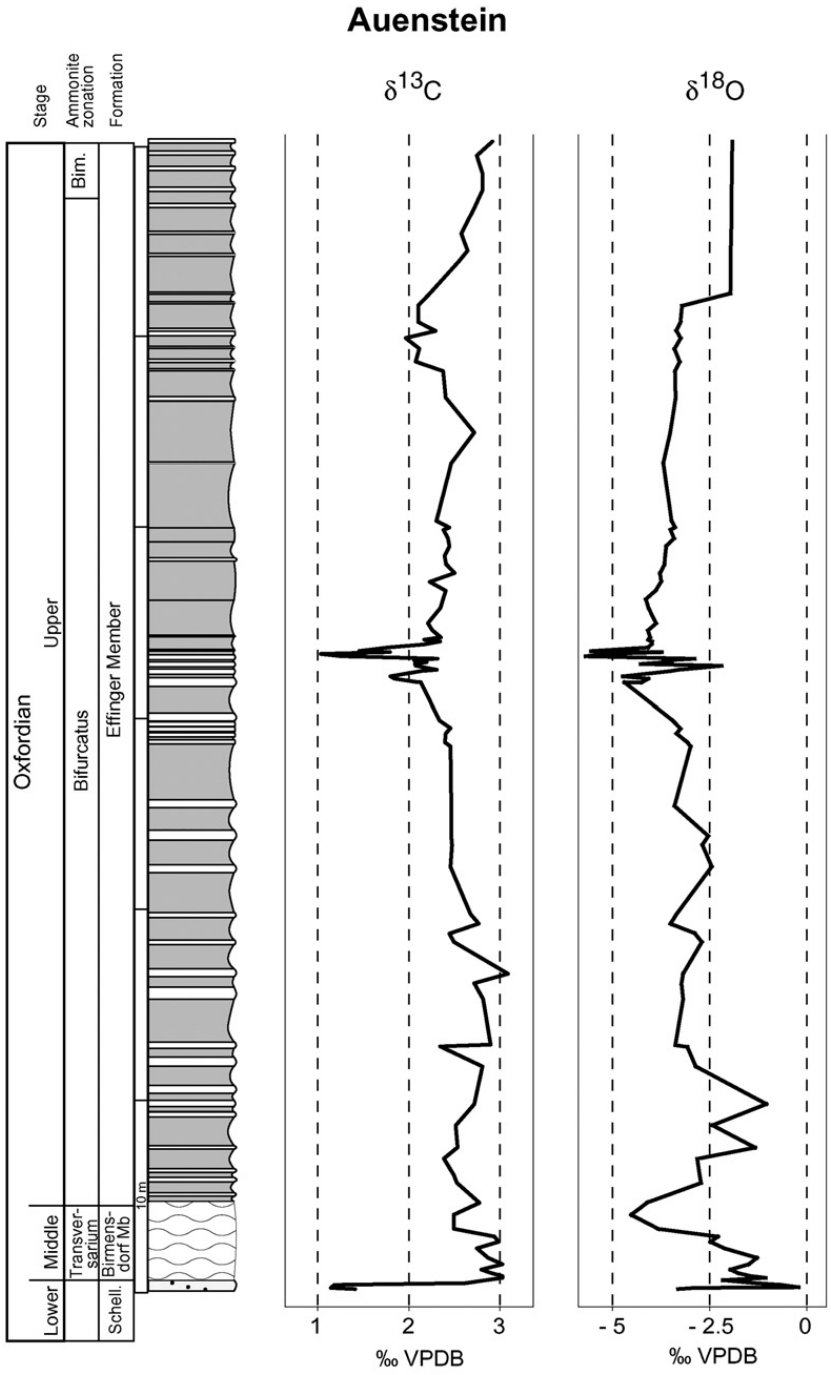

Fig. 3. Lithology, stratigraphy and carbon and oxygen stable isotopes of the Auenstein section. Biostratigraphy based on Gygi (2000). The isotopic curve is a compilation of Padden et al. (2002) and our own measurements.

bryozoans, bivalves, sponges and serpulids. The top of the bed is covered by a stromatolitic crust. Thin-bedded micritic limestones and marlstones of the overlying Birmensdorf Member contain micritic limestone nodules, algae, sponges and pelagic fauna (mainly ammonites). The first 50 cm of this Member are rich in fossil shells and glauconitic pebbles. The Effinger Member with its thin-bedded succession of alternating marlstones and limestones is similar to the Effinger Member in Weiach. According to Gygi (1986), the boundary between the Birmensdorf and Effinger Members corresponds to the transition from the Transversarium to the Plicatilis ammonite Zone. The correlation between the regional biostratigraphy (Gygi and Persoz, 1986; Gygi, 2000) and the usual Tethyan zonation was established by Louis-Schmid et al. (2007), by using carbon-isotope stratigraphy. In this paper, all ammonite zones refer to the Tethyan zonation.

2.3. Nissibach

Nissibach is located in the Helvetic tectonic unit near Walenstadt. This section is composed of sediments accumulated along a more distal part of the northern Tethyan shelf (Fig. 4). The studied succession starts with a 100 cm-thick bed described as Blegi–Oolith, which consist of a limestone rich in iron ooids and fossils, and covered by a hardground (Dollfus, 1961; Kugler, 1987; Burkhalter, 1995). The overlying lithology, the Schilt Limestone, is a micritic nodular limestone containing planktonic foraminifera, ammonites and belemnites. The end of the Blegi–Oolith is dated as Early Callovian, and the onset of the Schilt Limestone as Middle Oxfordian (Transversarium Zone). The sedimentation gap between the two formations covers several ammonite zones (Dollfus, 1961; Kugler,

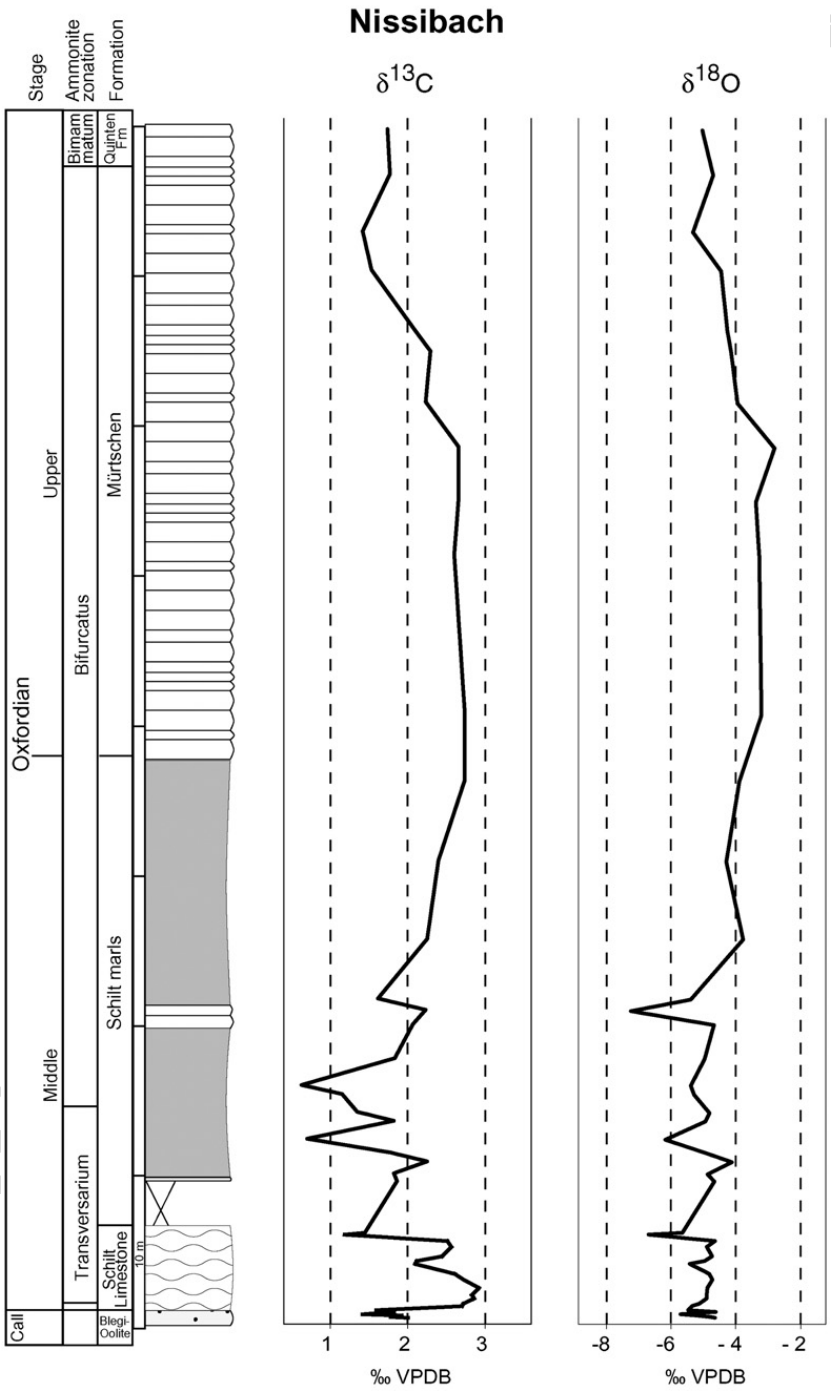

Fig. 4. Lithology, stratigraphy and carbon and oxygen stable isotopes of the Nissibach section. Biostratigraphy based on Kugler (1987). The isotopic curve is a compilation of Padden et al. (2002) and our own measurements.

1987). The last part of the Oxfordian is represented by the dark-grey Schilt Marls, followed by the Mürtschen Member, a well-bedded grey limestone.

2.4. Gantrisch

The Gantrisch section (Fig. 5) is located in the Middle Penninic "Prealpes Medianes" tectonic unit. Palaeogeographically this area was part of the Briançonnais, a submarine high located southeast of the Iberian microplate during the Jurassic. Based on the description of Furrer (1979), Homewood and Winkler (1977), and Winkler (1977), we have divided the Gantrisch section in three parts: the Formation Calcaréo-argileuse, the Knollenkalk and the Malmkalk. The Formation Calcaréo-argileuse is a monotonous marl with thin-shelled bivalves and scarce echinoderm debris. The Knollenkalk is a micritic nodular limestone that contains planktonic foraminifera, calcispheres and thin-shelled bivalves. Furrer (1979) defined the Knollenkalk as Middle

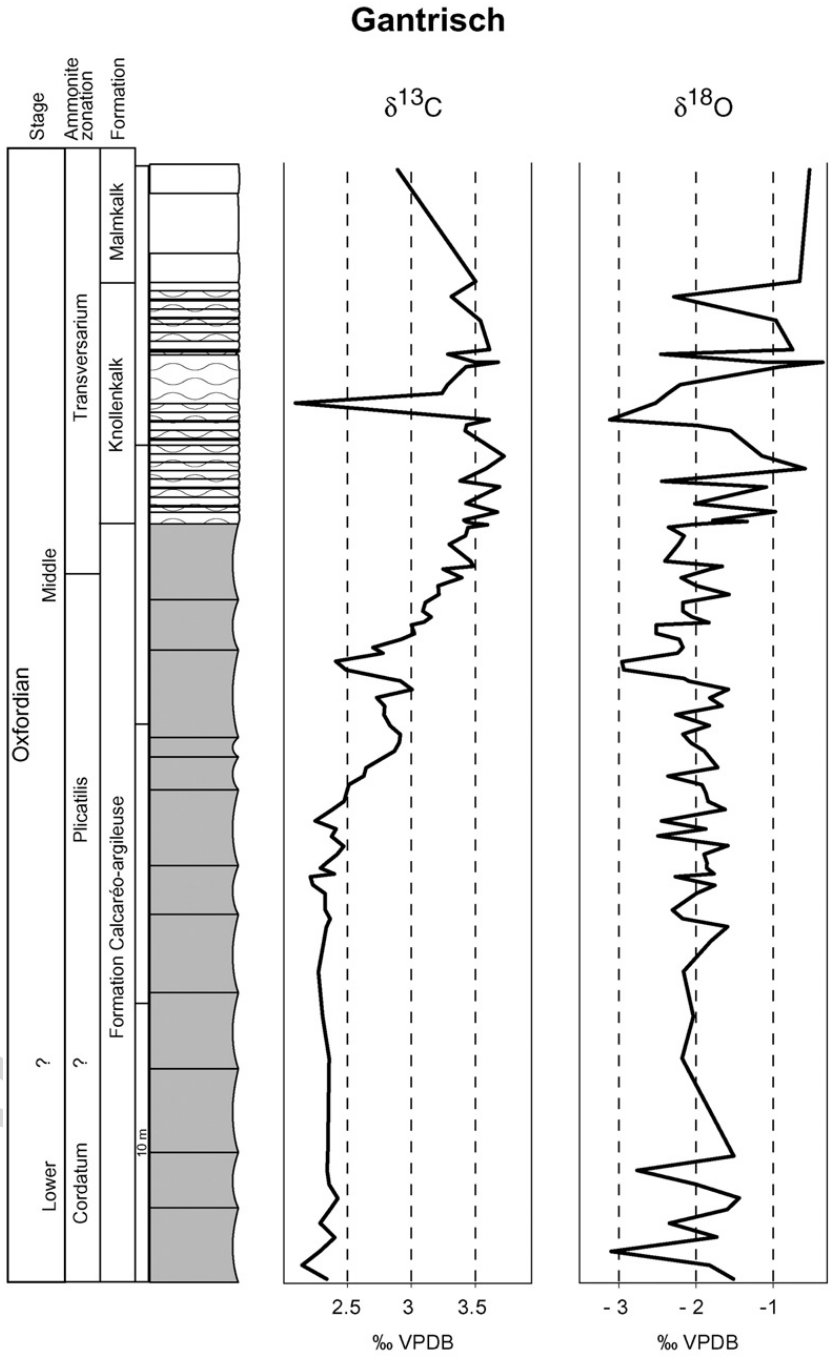

Fig. 5. Lithology, stratigraphy and carbon and oxygen stable isotopes of the Gantrisch section. Biostratigraphy based on Furrer (1979).

Oxfordian in age, whereas the remainder of the Upper Jurassic is represented by the Malmkalk, a thick succession of white micritic limestones.

3. Materials and methods

Sediment description is based on field observation combined with thin section analyses. Further investigations were done by cathodoluminescence microscopy. Samples for carbon isotope analysis were taken at intervals ranging from 5 cm in the hardgrounds to 50 cm in the non-condensed parts. Powders were produced by using a micro-drill to avoid crack fillings, fossils or irregularities especially in hardgrounds. In nodular limestones, samples were obtained from the nodules rather than from the matrix, because they are less diagenetically altered (for more details, see below).

The oxygen and carbon isotope composition of bulk-rock was analyzed with a VG-Prism mass spectrometer fitted with an automated Isocarb common acid bath preparation system. The mass spectrometer was calibrated with NBS 19, NBS18 and NBS20. The isotopic compositions are reported in the conventional delta-notation with respect to VPDB. Analytical reproducibility is better than ±0.1‰ for both carbon and oxygen.

Inorganic carbon and total carbon contents were measured on a UIC CM5012 Coulometer. Organic carbon contents were calculated by difference. Organic and inorganic carbon contents are expressed in weight percent carbonate. Analytical precision is ±0.1 wt.% for carbonate carbon and ±0.3 wt.% for organic carbon.

4. Lithological and geochemical characteristics of Callovian and Oxfordian sediments

4.1. The "Anceps–Athleta Bed", the "Schellenbrücke bed", and the "Blegi–Oolith"

The Callovian and the Lower Oxfordian in Weiach, Auenstein and Nissibach are characterized by intermittent sedimentation and long sedimentary gaps (Dollfus, 1961; Gygi and Persoz, 1986; Kugler, 1987; Matter et al., 1988). The sediments deposited during this period show a variety of unusual sedimentologic features related to low accumulation rates and characteristic of hardgrounds and condensed sediments (Gygi, 1981; Gehring, 1986; Kugler, 1987; Burkhalter, 1995), such as thorough bioturbation, reworked intraclasts, concentration of fossils, encrusting organisms, enrichment with glauconite and iron mineralization.

In Weiach, the "Anceps–Athleta Bed" is a 1.6 m thick alternation of dark grey marls and grey limestones. The limestone beds are 5 to 20 cm thick and consist of a bioturbated wackestone to packstone, with around 70 wt.% carbonate. The dark grey marls have the same range of bed thickness. Their carbonate content is around 20 wt.%, and the organic carbon content is up to 0.7 wt.%. The extraclasts embedded in the carbonate matrix consist mainly of iron ooids and pelagic fossils, which are irregularly distributed in a micritic matrix. The iron ooids are abundant and are generally composed of a nucleus of quartz, bioclast or a broken-piece of iron-ooid, surrounded by circular layers, which mainly consist of chamosite (Matter et al., 1988) (Fig. 6A). Their diameter is usually around 0.5 mm, but can reach up to 1.5 mm, especially when the center consists of an assemblage of several smaller ooids. Macrofossils consist exclusively of ammonites and belemnites. They are occasionally covered by a limonitic crust or have microboring features. Belemnites are sometimes enriched in pockets. In the Weiach core, a cluster of eight belemnites was found (Fig. 6A). The microfossils are represented by a few planktonic foraminifera, calcareous thin-shelled bivalves and echinoderm fragments. Quartz grains, glauconite and cavities filled with calcite crystals were also observed.

In Auenstein, the "Schellenbrücke bed" is a 50 cm-thick limestone bed, of red, yellow or green color (Fig. 6B). It consists of a packstone, rich in bioclasts and iron ooids. Bioclasts are dominant and iron ooids are less abundant compared to Weiach. The structure of this bed is very irregular with intraclasts up to several centimetres in size. Cavities of up to several centimetres in diameter, filled with sparry calcite, are distributed throughout the bed. Iron mineralization crusts up to 2 mm thick have also been observed. The majority of the macrofauna is pelagic and consists of up to 80% ammonites and belemnites (Gygi and Persoz, 1986). Echinoderms, bivalves, bryozoans, sponge fragments and algae were also observed. The bioclasts and the lithoclasts are frequently covered by a limonitic crust and perforated by benthic organisms. Several kinds of encrusters like serpulids and encrusting foraminifera have also been identified. In Auenstein, stromatolitic crusts usually cover the top of the bed (Fig. 6B), and are also found around the lithoclasts and as erosive horizons traversing the bed. They consist of a thin-laminated green layer, which is up to 1 cm-thick. A small amount (<1%) of detrital quartz has also been observed.

The "Blegi–Oolith" of Nissibach is a 100 cm thick bed also containing iron ooids. The Blegi–Oolith consists of a biomicritic limestone with an irregular distribution of the components in the matrix (mudstone to packstone), due to the presence of bioturbation and

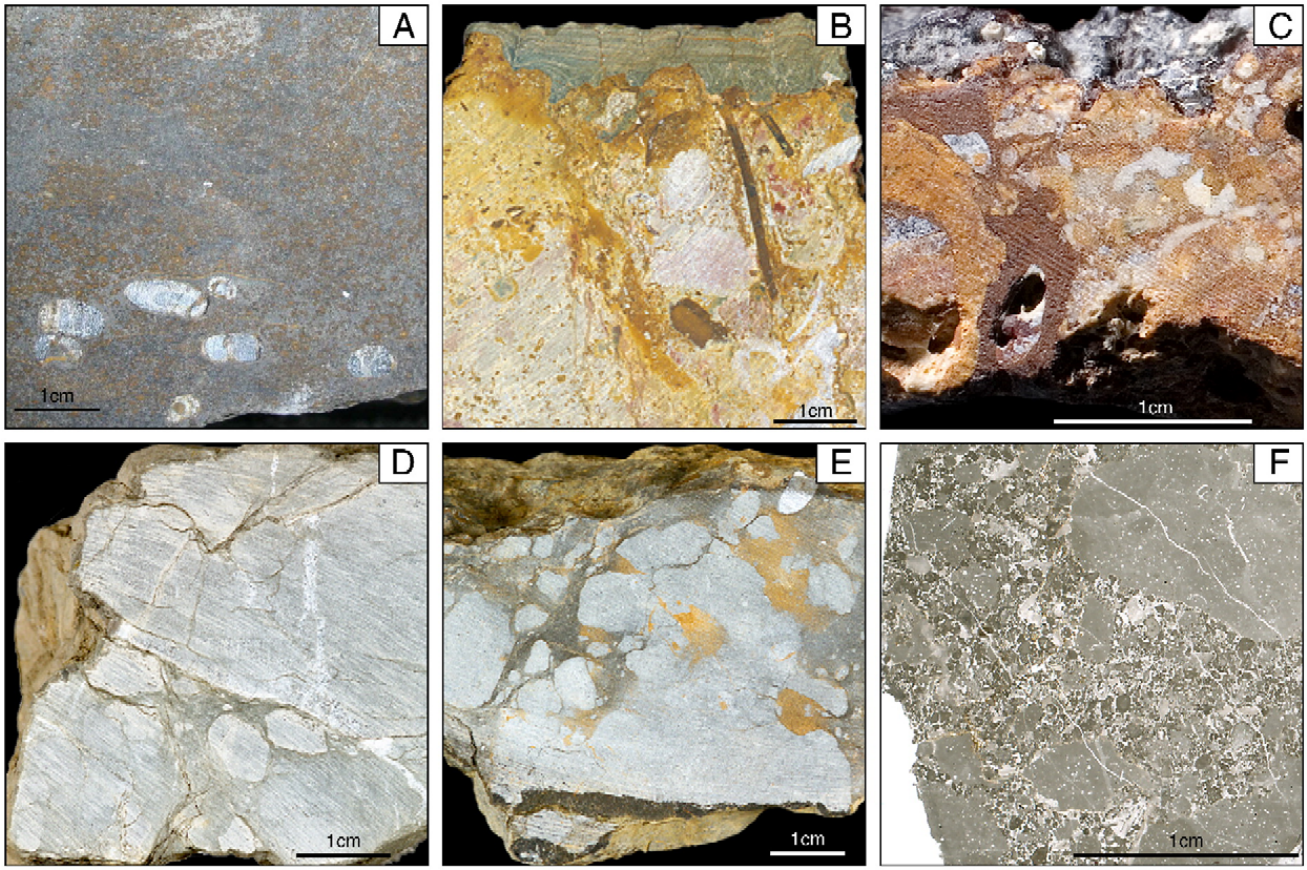

Fig. 6. Pictures of condensed beds and nodular limestones. A: Condensed bed from Weiach with iron ooids (brown dots). Seven belemnites are regrouped at the base of this sample. B: The Schellenbrücke Bed from Auenstein. The top of the bed is covered by a green stromatolitic crust. C: Modern hardground formed by scouring of oceanic currents. Marion Plateau, Australia. D: Nodular limestone from Gantrisch. Stylolites are commonly found around nodules. E: Nodular Schilt limestone from Nissibach. F: Thin-section of the Gantrisch nodular limestone. In this sample, the matrix between the micritic nodules consists of a sparitic, shallow-water limestone.

intraclasts. The red, yellow or green coloration of the sediment attests of the presence of iron, which is also concentrated in glauconitic pebbles, mineralized crusts, and iron ooids. The distribution of iron ooids is irregular. In some areas, they represent 90% of the components, whereas they are scarce in other places. The bioclasts are less abundant than in Auenstein. Also here, cephalopods dominate the macrofauna. The remaining fossils include globigerinoids, echinoderm fragments, sponge spicules, calcispheres. Stromatolites form thin layers of 1 mm thickness. They encrust cemented sediment and bioclasts. The detrital content is low, quartz grains represent <1% of the components. Cavities partly or totally filled with coarse, sparry calcite crystals were observed either within the sediment or in shells. Their size varies from a few millimetres to two centimetres.

4.2. Nodular limestones

Above the hardgrounds, a nodular limestone facies of variable thickness is observed in Auenstein (5 m), Nissibach (6 m) and Gantrisch (12 m) (Fig. 6D, E, F). It consists of decimetre- to metre-thick bedded limestones. Nodules are similar in the three locations, and consist of a mudstone with pelagic fossils and a few echinoderm and sponge clasts. The pelagic fauna consists mainly of planktonic foraminifera (globigerinoids), belemnites and ammonites. Between the nodules, the matrix is composed of micritic to microsparitic iron-rich calcite with few unidentified bioclasts. The carbonate content is higher in nodules (91% on average) than in the surrounding sediment (68% on average). The nodule size, shape and distribution can be heterogeneous vertically and horizontally. Their diameters vary from a few millimetres to several centimetres. They are usually sub-rounded and the boundary with the surrounding matrix is mostly sharp and often marked by the presence of stylolites. An ammonite shell is occasionally delimiting the border of nodules. Sometimes nodules are covered by encrusting organisms, indicating a subaquatic exposure at the sediment surface. One sample in Gantrisch shows typical

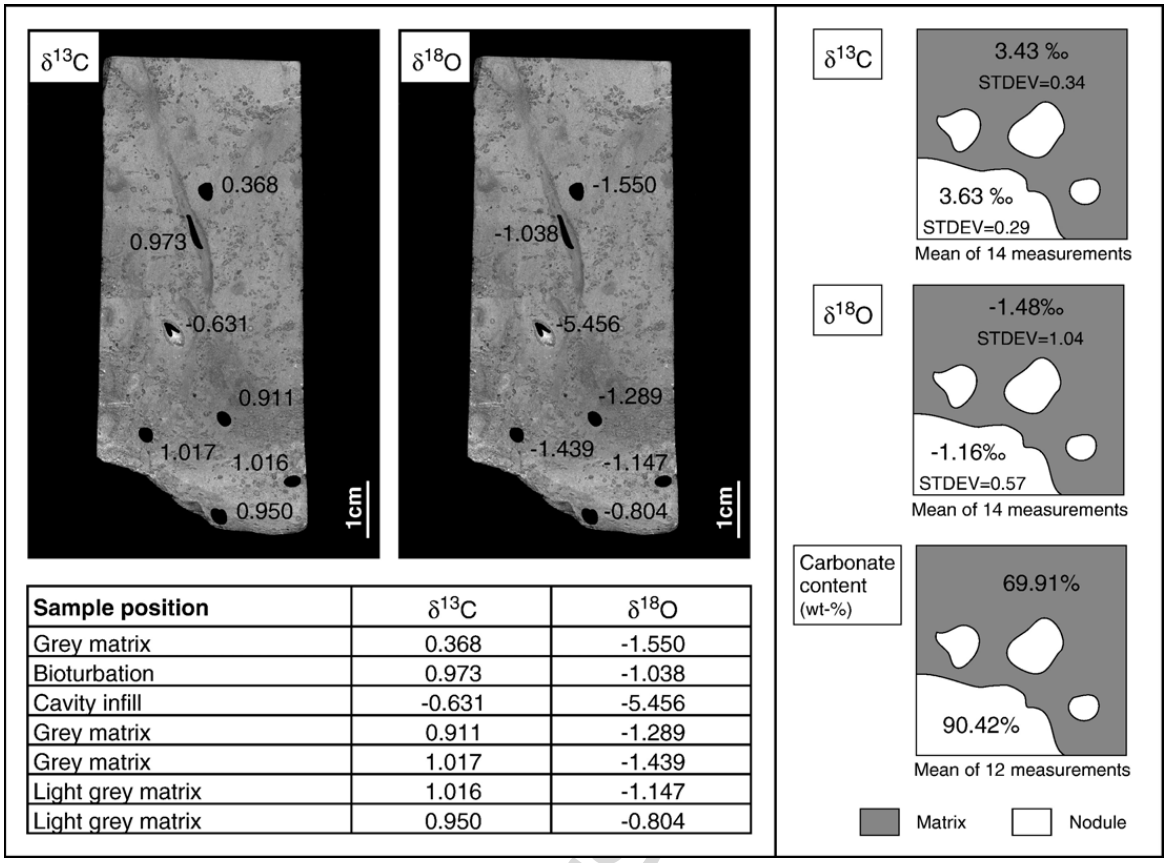

Sample position	$\delta^{13}C$	$\delta^{18}O$
Grey matrix	0.368	-1.550
Bioturbation	0.973	-1.038
Cavity infill	-0.631	-5.456
Grey matrix	0.911	-1.289
Grey matrix	1.017	-1.439
Light grey matrix	1.016	-1.147
Light grey matrix	0.950	-0.804

Fig. 7. Left part: Carbon and oxygen isotope measurements on condensed lithologies. Example of the Anceps–Athleta Bed from Weiach. Right part: Average values of carbon and oxygen isotopes, and carbonate content from the Gantrisch nodular limestone.

hemipelagic nodules, surrounded by a sparitic matrix with shallow-water clasts composed of pellets, miliolids and aggregate grains.

4.3. Isotopic measurements on hardgrounds and nodular limestones

Oxygen and carbon isotopes were measured on 44 different components of the hardgrounds from Auenstein and Weiach, and another 34 samples were analyzed on nodular limestones. An example from the Anceps–Athleta Bed from Weiach and a compilation of the data on the Gantrisch nodular limestones are shown in Fig. 7.

The analyses of carbonate from the hardgrounds reveal that, within one sample, the $\delta^{13}C$ and $\delta^{18}O$ measured in the micritic matrix are homogeneous, whereas cavity infills show $\delta^{18}O$ values ranging between −5.4‰ and −7.9‰. Carbon isotope compositions of the micritic matrix range between 0.3‰ and 1.6‰, depending on the sample and its position in the hardground. The oxygen isotope composition of bulk rock shows in average less negative values in the hardgrounds than in the upper part of the section. In Weiach $\delta^{18}O$ values range from −.6‰ to −3.6‰ in the Anceps–Athleta Bed, and from −2.5‰ to −4.1‰ in the Birmensdorf and Effinger Members (Fig. 2).

The nodular limestones have similar $\delta^{13}C$ and $\delta^{18}O$ in the nodules and in the encasing lithologies (Figs. 3–5). Only a small difference of $\delta^{13}C$ and $\delta^{18}O$ between nodules and the surrounding matrix is observed (Fig. 7). The nodules have a carbon-isotope composition in average 0.2‰ higher than the matrix. For oxygen isotopes, nodules are up to 1.17‰ less negative (0.32‰ in average).

5. Carbon and oxygen isotope stratigraphy

5.1. Carbon and oxygen data from the studied sections

Carbon and oxygen isotope results are presented in Figs. 2–5 and carbon isotopes are graphically summarized in Fig. 8. In Weiach, Auenstein and Nissibach, the measured carbon isotope record starts with a sharp positive shift of more than 1.5‰ (Figs. 2–4). The most positive values recorded in the sediments situated just above the hardgrounds fall within a range of 2.8‰ to 3.3‰. The upper part of the carbon isotope curve shows values between 1‰ and 3‰. The shift to lower values in the Auenstein and Nissibach sections are discussed by

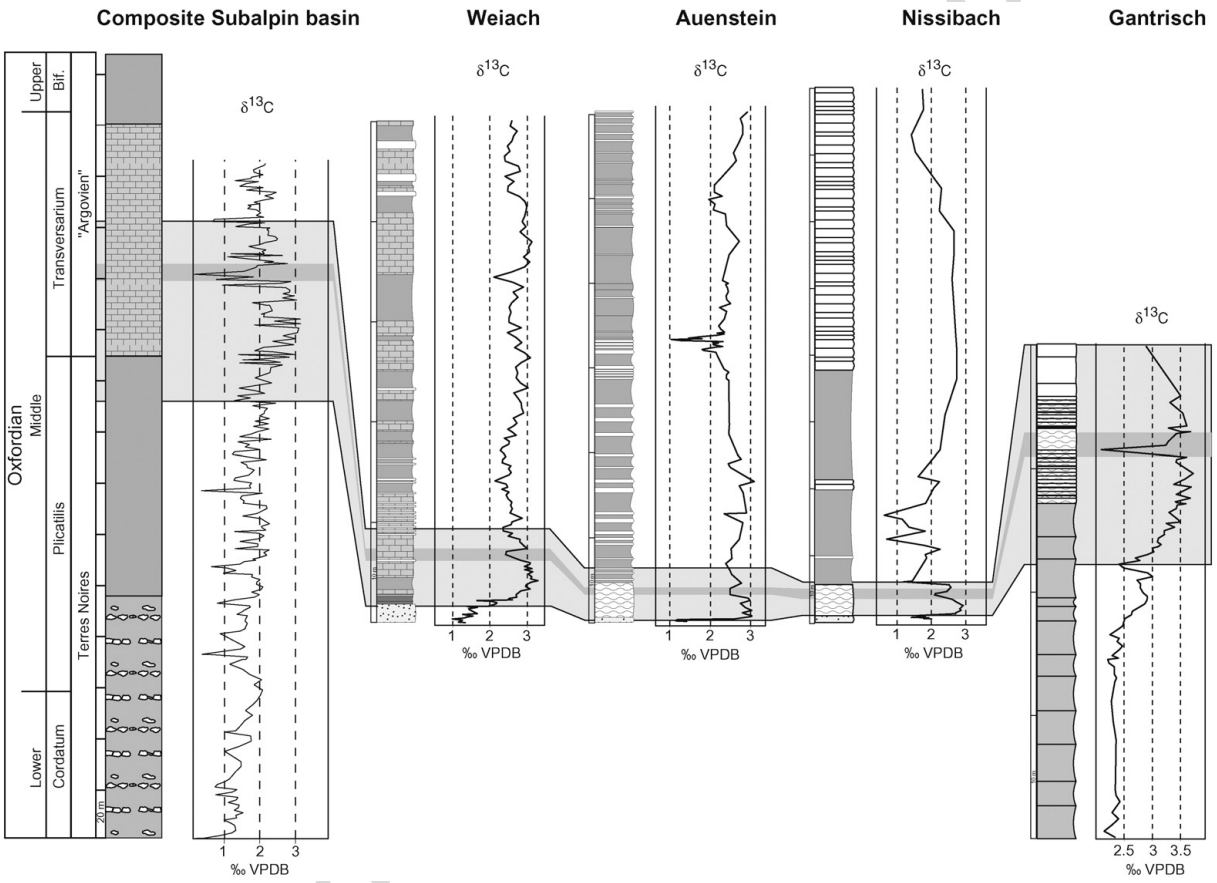

Fig. 8. Correlation of the studied sections and the reference section from the Subalpine Basin (Louis-Schmid et al., 2007). The light-grey zone corresponds to the Plicatilis–Transversarium positive excursion, the dark-grey zone represent the interval marked by lower values within the positive excursion.

Padden et al. (2001) and Louis-Schmid (2006). In Gantrisch, the values increase progressively from 2.3‰ in the Formation Calcaréo-argileuse to a maximum of 3.7‰ within the Knollenkalk. The oxygen isotope values fluctuate between −3‰ and −0.5‰ in the sediments from the sections Weiach, Auenstein and Gantrisch ((Figs. 2,3,5)). The section Nissibach shows more depleted $\delta^{18}O$ values, ranging from −6‰ to −4‰ (Fig. 4).

5.2. Reference section for carbon-isotope stratigraphy

We compare the established carbon isotope records with a high-resolution carbon-isotope curve from southeastern France (Fig. 8), where an accurate ammonite stratigraphy was established (Gaillard et al., 1996; Pellenard, 2003; Gaillard et al., 2004). Here we only summarize the most important characteristics of this section, a detailed description can be found in Louis-Schmid et al. (2007). The isotopic record was established on a composite section from the eastern part of the Subalpine Basin. The Callovian–Oxfordian deposits correspond to the uppermost part of the "Terres Noires", a succession of marlstones punctuated by rust-colored limestone beds (Pellenard et al., 1999). The rapidly subsiding Subalpine Basin corresponds to a sedimentary sink with high sedimentation rates. High sedimentation rates, carbonate contents of more than 40% (Louis-Schmid et al., 2007) and a rich ammonite fauna make it a good reference section for carbon-isotope stratigraphy.

Most remarkable in the carbon-isotope record from the composite Subalpine Basin section is a positive $\delta^{13}C$ excursion culminating at 3.1‰ in the Transversarium ammonite Zone (Louis-Schmid et al., 2007). A short excursion towards values near 1‰ marks the end of the positive carbon isotope anomaly. The upper part of the carbon isotope curve shows a decreasing trend of the values from 2.5‰ to 2‰.

6. Discussion

6.1. The Callovian–Oxfordian sedimentation

The Callovian and the early part of the Oxfordian was a time of intermittent sedimentation and erosion, which resulted in the formation of hardgrounds. These hardgrounds, which consist of a few tenths centimetres of sediments in the studied sections, are the only archives of a period estimated at about six million years (Gradstein et al., 2004). Sedimentological, geochemical and palaeontological evidences indicate that these hardgrounds are of a submarine origin and were formed in an outer-shelf to upper slope environment. The presence of encrusting organisms, iron impregnations and mineralization of iron crusts confirm that they were exposed for a long period at the sea floor surface.

The processes which might trigger the formation of hardgrounds include: (1) extreme dissolution of carbonates at the sea floor (Garrison and Fischer, 1969; Schlager, 1974), (2) low sediment input from platforms and emerged lands (Schlager, 1989; Dromart, 1992), (3) scouring of the sea floor by bottom currents (Fuersich, 1979). A strong dissolution can be excluded for the following reasons: First, the fossils observed are well preserved, even thin-shelled fossils and they do not present evidence for strong dissolution. Moreover, the bathymetry was too shallow to fall below the aragonite or calcite compensation depth. Auenstein sediments were accumulated at an estimated depth of 100 m below sea level (Gygi and Persoz, 1986).

Rapid sea-level variations can result in a decrease of sediment input to the deposition area, by emergence or drowning of the sediment source region, or by local changes in sediment distribution patterns. However, the duration of the Callovian–Oxfordian condensation event, lasting for about six million years (Gradstein et al., 2004), is too long to be explained only by sea-level variations. Furthermore, the presence of bioclasts and quartz grains in the hardgrounds indicates that there was at least intermittent sediment supply to the seafloor.

The last hypothesis to be tested is that strong oceanic currents were sweeping the seafloor of the northern Tethyan margin and were removing the particles from the exposed area. This model is more realistic considering the time involved in the condensation event, as oceanic currents can be active for several millions of years. Moreover, the general distribution pattern of sediments is also concordant: the particles were winnowed from the area exposed to currents, i.e. the upper slope and the shelf, whereas deeper basins collected the particles. This explains the high accumulation rates of the Subalpine Basin. Three sedimentological features suggest an important current activity: a) reworked hardground fragments redeposited as intraclasts, b) the presence of rounded iron ooids (Burkhalter, 1995) and c) fossils, which were transported and accumulated at the same place.

In order to confirm this hypothesis, we compared the Oxfordian hardgrounds with modern hardgrounds forming under comparable conditions. The Marion Plateau offshore NE Australia (ODP leg 194), and the Great Australian Bight "shaved shelf" (James et al., 2001) are two examples of recent hardgrounds forming

under strong oceanic currents in a rather shallow carbonatic environment. In the southern Marion Plateau, the elevated topography combined with strong bottom currents (up to 2.5 m/s) prevents sedimentation of particles. Hardgrounds were formed since the Late Miocene/Early Pliocene (Isern et al., 2001). Pieces of the submarine hardground, situated at 117 m and 300 m water depth, were recovered by dredging (Fig. 6C). The hardground dredged from the Marion Plateau is a 3 cm-thick crust, which shows features similar to the Jurassic hardgrounds. First, iron imparts the same yellowish and reddish colors to the sediment. The bed consists of biomicritic carbonate clasts covered by a laminated crust, very similar to the stromatolites of Auenstein and Nissibach. The crust is extensively colonized by serpulids, bryozoans and solitary corals. The carbonate clasts contain abundant planktonic foraminifera and bioclasts from bryozoans, mollusks and corals (Heck et al., in preparation). The hardground contains many cavities very similar to the ones of the Jurassic hardgrounds, except that they have no diagenetic infill. The time involved is also comparable, with lacking of sedimentation during 5 Myr.

James et al. (2001) investigated sedimentation patterns along the Great Australian Bight. They identified widespread palimpsest deposits and reduced carbonate sedimentation due to the strong and complex influence of oceanic currents along the shelf-edge. The resulting palimpsest sediments are also similar to the Jurassic hardgrounds, with calcareous relict intraclasts and biofragments. The intraclasts are enriched in iron (goethite and chamosite). The hard substrates are colonized by encrusting fauna, mollusks, sponges, and bryozoans, but the sediment generated there is swept away by strong currents. The sediment repartition pattern is distinctive on different sectors of the shelf, with areas protected from currents where sediment accumulates, and exposed areas where the particles are winnowed. The Great Australian Bight can be taken as a modern analogue of the northern Tethyan margin during the Oxfordian. The sections of Weiach, Auenstein and Nissibach correspond to the exposed areas and therefore recorded a hardground and Gantrisch would correspond to a local basinal area protected from the current effect, where sediment could settle.

6.2. Nodular limestones

Several models have been developed to explain the formation of the nodular fabrics (see Fluegel, 2004 for a recent review). The only common condition thought to lead to nodular fabric is a low sedimentation rate. Based on an investigation of modern intraclasts formation on the Bahamas, Mullins et al. (1980) suggest that the nodular limestones are formed under fluctuating oceanic current activity. The current, in a first stage, supplies the necessary ions for the early cementation of the carbonate ooze by creating a flux of water moving through the sediment. After that, intraclasts are formed and reworked by a combination of bioturbation and current action, which creates the nodular fabric. This model is in agreement with our own observations: the numerous ammonites indicate a slightly condensed episode, nodules were obviously reworked and are sometimes covered by encrusting organisms, which shows that they were exposed at the seafloor. However, another process has to be added to this model to explain the angular shape of some intraclasts and the sample from Gantrisch, which is composed of pelagic nodules surrounded by a shallow water matrix (Fig. 6D,E,F). We propose that, in addition to the early cementation of carbonate ooze by the action of currents and bioturbation, there was a remobilization of the intraclasts and a regular sediment transport from a carbonate platform to deeper settings. This model explains the variable shape of the intraclasts, depending on their degree of cementation before the remobilization, but also the coarser grained matrix surrounding the nodules. Similar resedimentation processes have been observed on the Little Bahama Bank (Lantzsch et al., 2005). The structure of the redeposited sediment is comparable to the nodular limestones with cemented fine-mud pebbles surrounded by a coarser matrix.

6.3. Carbon isotope stratigraphy

Previous biostratigraphic work on the studied sections indicated a Middle Oxfordian age for the first sediments overlying the hardgrounds. According to Gygi (2000) in Auenstein and Kugler (1987) in Nissibach, the nodular limestones are part of the Transversarium ammonite Zone. Likewise the nodular limestones of the Gantrisch section are dated as middle Oxfordian by Furrer (1979). To improve the accuracy of the correlation between the different sections, we used carbon isotope stratigraphy in addition to biostratigraphy.

Before discussing the use of the carbon isotopes for stratigraphy, we have to exclude an influence of diagenesis on the measured samples. In Weiach, Auenstein and Gantrisch, $\delta^{18}O$ values (Figs. 2,3,5) indicate a moderate diagenetic overprint. Therefore, oxygen isotopes cannot be used as a palaeotemperature proxy. The section Nissibach shows more negative $\delta^{18}O$ values (Fig. 4) due to the tectonic position of the section, which suffered a strong

burial diagenesis during the formation of the Alps. The carbon-isotope composition, which is less sensible to high burial temperature than oxygen-isotopes, did not suffer a strong diagenetic overprint and preserved the original trend, even in Nissibach (Padden et al., 2002). Moreover, we consider that a strong diagenetic influence on the studied sections can be excluded for the following reasons: a) microfossils are well preserved and show no evidence for recrystallization. b) a covariance between the carbon and the oxygen isotope records is lacking (Figs. 2–5). c) the carbon isotope records show an excellent correlation across depositional environments and lithologies (Figs. 2–5). The robustness of the $\delta^{13}C$ signal is supported by the overlapping curves of the five different sections. The Gantrisch carbon-isotope record proves that the isotopic signal is clearly not linked to lithological changes. There, the positive excursion starts one metre below a lithological boundary and the curve does not mirror the transition from marls to nodular limestones.

Seafloor cementation and early diagenesis can influence oxygen and carbon isotope signals (see Mutti and Bernoulli, 2003 for a recent review). Oxygen isotopes measured on the studied hardgrounds could reflect the effect of a seafloor cementation, which produce isotopically heavier cement due to cooler bottom water temperatures (Mutti and Bernoulli, 2003). The $\delta^{13}C$ is generally less affected by seafloor cementation than $\delta^{18}O$ (Marshall and Ashton, 1980; Aghib et al., 1991). Isotopic measurements performed on cavity infills indicate a late-diagenetic alteration (Fig. 7) (Mettraux et al., 1989). Therefore, only the measurements on the micritic matrix reflect an original marine carbon isotope signal (Cecca et al., 2001). In conclusion, the isotopic values measured on the hardgrounds should be taken with some caution, and therefore, in this study, the age of the hardgrounds is based on ammonite stratigraphy. The specific analyses performed on nodular limestones reveal that carbon and oxygen isotope results were not influenced by seafloor cementation. The very small difference of $\delta^{13}C$ and $\delta^{18}O$ between the nodules and the surrounding matrix (Fig. 7) is probably due to the difference in carbonate content between the nodules and the matrix (Fig. 7). The lower carbonate content of the matrix makes it more sensible to diagenetic overprinting. Therefore, we always used nodule samples for the construction of the carbon isotope curve.

The mid-Oxfordian positive $\delta^{13}C$ excursion, already documented by Jenkyns (1996) and Weissert and Mohr (1996), could be reproduced in all the studied sections. The large amplitude shift of the carbon-isotope curve enables a good correlation with the composite Subalpine Basin section (Fig. 8). The high frequency variations of the $\delta^{13}C$ record and their reproducibility allowed us to identify an interval marked by lower values within the positive excursion and to use this interval for correlation (dark-grey zone, Fig. 8). Based on the correlation with the biostratigraphically dated C-isotope curve of the Subalpine Basin we can demonstrate that post-hardground sedimentation started towards the end of the Plicatilis ammonite zone and that the change in sedimentation is synchronous in the four studied sections.

6.4. Sedimentation and current history of the northern Tethyan margin

The sedimentary sequence described above shows that strong shelf currents were active along the northern Tethyan margin creating hardgrounds similar to the ones forming today on the Marion Plateau or along the Great Australian Bight "shaved shelf". Hardgrounds were formed on the exposed seafloor, whereas deeper basins or protected areas collected sediment particles winnowed by currents. We interpret the nodular limestones immediately following the hardgrounds as an expression of a last pulse of oceanic current activity marked by decreasing intensity. This phase is followed by the deposition of marls and carbonate ooze, which mark the onset of the significant accumulation of carbonates in Late Jurassic oceans.

By combining bio- and chemostratigraphy, we were able to reconstruct an accurate time frame of the depositional events (Figs. 8 and 9). Three different depositional histories can be identified from the sections: a) a continuous sedimentation in deep protected areas in the Subalpine Basin, b) a strong sediment-starved phase on the sections exposed to currents (Weiach, Auenstein, Nissibach) and c) for Gantrisch an intermediate evolution.

The Subalpine Basin was protected from currents by its morphology and its depth. The deposition was continuous from Late Callovian to Middle Oxfordian, there is no sedimentary or chemostratigraphic evidence for hiatuses or current activity. On the contrary, the high accumulation rates for this period (Louis-Schmid et al., 2007) indicate that the Subalpine Basin acted as a sedimentary sink.

In the three sections of Weiach, Auenstein and Nissibach, hardgrounds were formed during the Callovian and Early Oxfordian. The onset of the current activity is provided by the age of the underlying lithologies, dated as Middle Bathonian to Lower

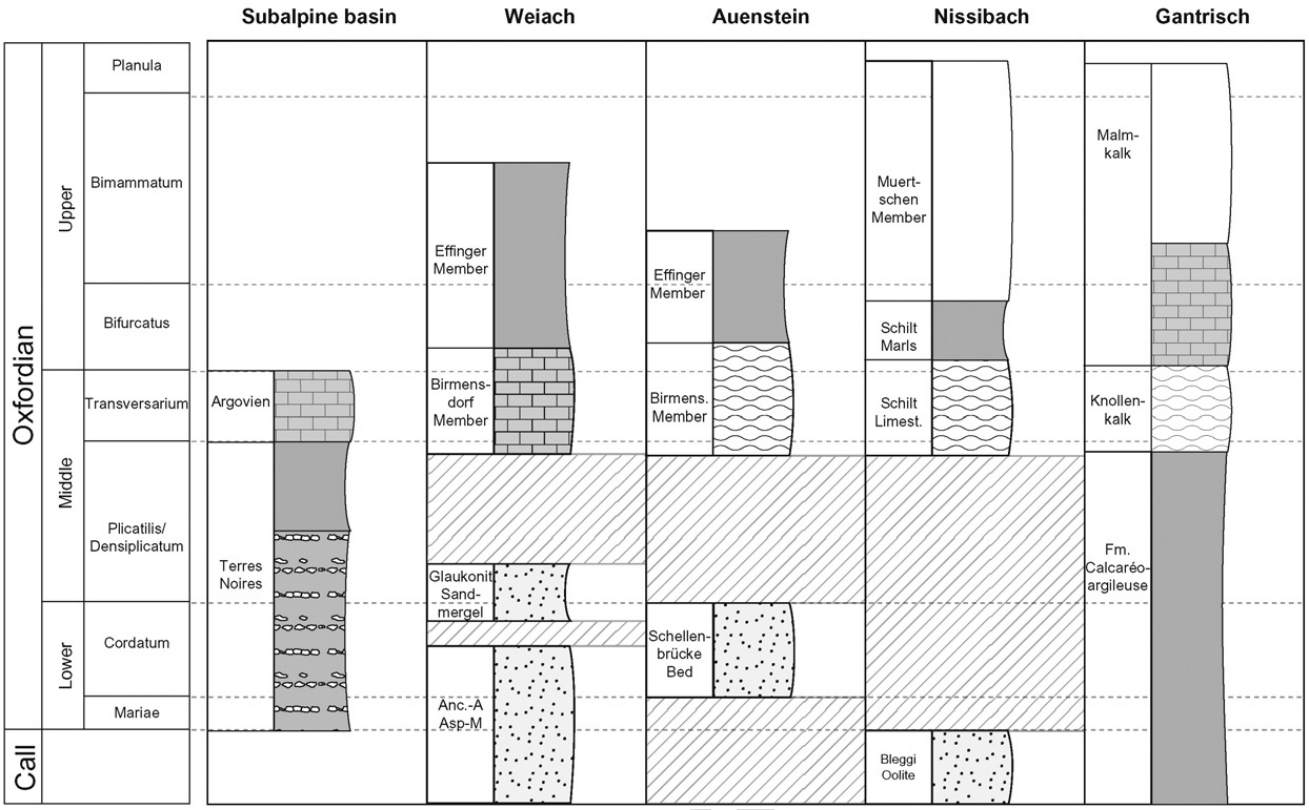

Fig. 9. Lithostratigraphical correlation. This figure is not to scale.

Callovian (Gygi and Persoz, 1986; Kugler, 1987; Matter et al., 1988). Shelf current intensity started to weaken at the end of the Plicatilis Zone and stopped within the Transversarium Zone. Our detailed carbon isotope stratigraphy allows to determine that this transition is synchronous in the three sections, although they are situated at different depositional sites. In Auenstein and Nissibach, the deposition of nodular limestones can be considered as a signature of decreasing current activity. In Weiach, the deposition of fine marls and limestones directly above the hardgrounds indicates that after the Plicatilis Zone, currents were also less effective at a greater palaeodepths.

C-isotope data indicate that the sediments of the studied Gantrisch section were accumulated in a local basinal setting on the northwestern Tethyan Briançonnais high, where deposition was apparently continuous until the Plicatilis Zone. The fine-grained marls from the Formation Calcaréo-argileuse were deposited in a low energy zone. However, this section is not necessarily representative for the whole Briançonnais High. Furrer (1979) reported other locations from the same area recording a hiatus and/or hardgrounds during that time. Therefore, Gantrisch was probably an area protected from the currents by a submarine topographic high. Nevertheless, this section records the nodular limestone unit, which indicates that a moderate current activity was forming nodules which later were redeposited an accumulated in the Gantrisch basin (Winkler, 1977). The onset of the nodular limestone deposition was synchronous with Auenstein and Nissibach.

6.5. Global evolution of oceanography and climate during the Callovian and the Oxfordian

The weakening of shelf current intensity along the northern Tethyan margin is only one of the changes, which occurred during the Middle Oxfordian. A variety of other climate and oceanography proxies indicate that the Oxfordian marks a turning point in Mesozoic palaeoceanography. Evidence for strong currents during the Callovian–Middle Oxfordian is not restricted to the alpine region. Similar sediments have been reported from several other geographical provinces all over the world: Tunisia (Cordey et al., 2005), Pakistan (Fatmi, 1972), India (Fuersich et al., 1992), Madagascar (Besairie and Collignon, 1971), Argentina (Legarreta, 1991).

Middle and Upper Jurassic radiolarites formed in pelagic settings of the western Tethys are interpreted as indicators of intense equatorial upwelling (Cottereau and Lautenschlager, 1994; Bombardiere and Gorin,

2000). Palaeontological evidence suggests that the transition from radiolarites to radiolarian limestones occurred during the Middle Oxfordian (Baumgartner, 1987), which suggests that weakening of equatorial upwelling coincided with waning of shelf currents.

Sea-level variations during this period are still debated. Some authors deduce a global transgression (Legarreta, 1991; Norris and Hallam, 1995), where others see an extreme regression (Dromart et al., 2003b). The Haq curve shows gentle second order variations within a first order transgressive trend (Fig. 10).

The time of widespread hardground formation coincided with cold global temperatures (Riboulleau et al., 1998; Abbink et al., 2001; Lécuyer et al., 2003). A stepwise warming starting in the Middle Oxfordian is documented by oxygen isotopes on belemnites from the Russian Platform (Fig. 10) and on fish teeth from the northern Tethys (Riboulleau et al., 1998; Wierzbowski, 2002; Lécuyer et al., 2003; Wierzbowski, 2004). Temperature change is also suggested by the migration of boreal ammonites to higher latitudes (Enay, 1980) and by palynological investigation in the southern North Sea (Abbink et al., 2001). The temperature increase was accompanied by an extension of the arid climate belt in the northern hemisphere, documented by evaporites and coal distribution (Hallam, 1985; Parrish, 1993), and by studies on palynology and clay mineralogy (Rioult et al., 1991; Abbink et al., 2001; Hautevelle, 2005).

The Middle Oxfordian climate warming associated with a general sea-level rise was favorable for the development of carbonate producing organisms (Leinfelder et al., 2002). First, on platforms, with the explosion of the number of reef sites and the diversity of reef builders (Fluegel, 2004) but also in pelagic environments with the expansion of calcareous nannofossils (Bartolini et al., 1996).

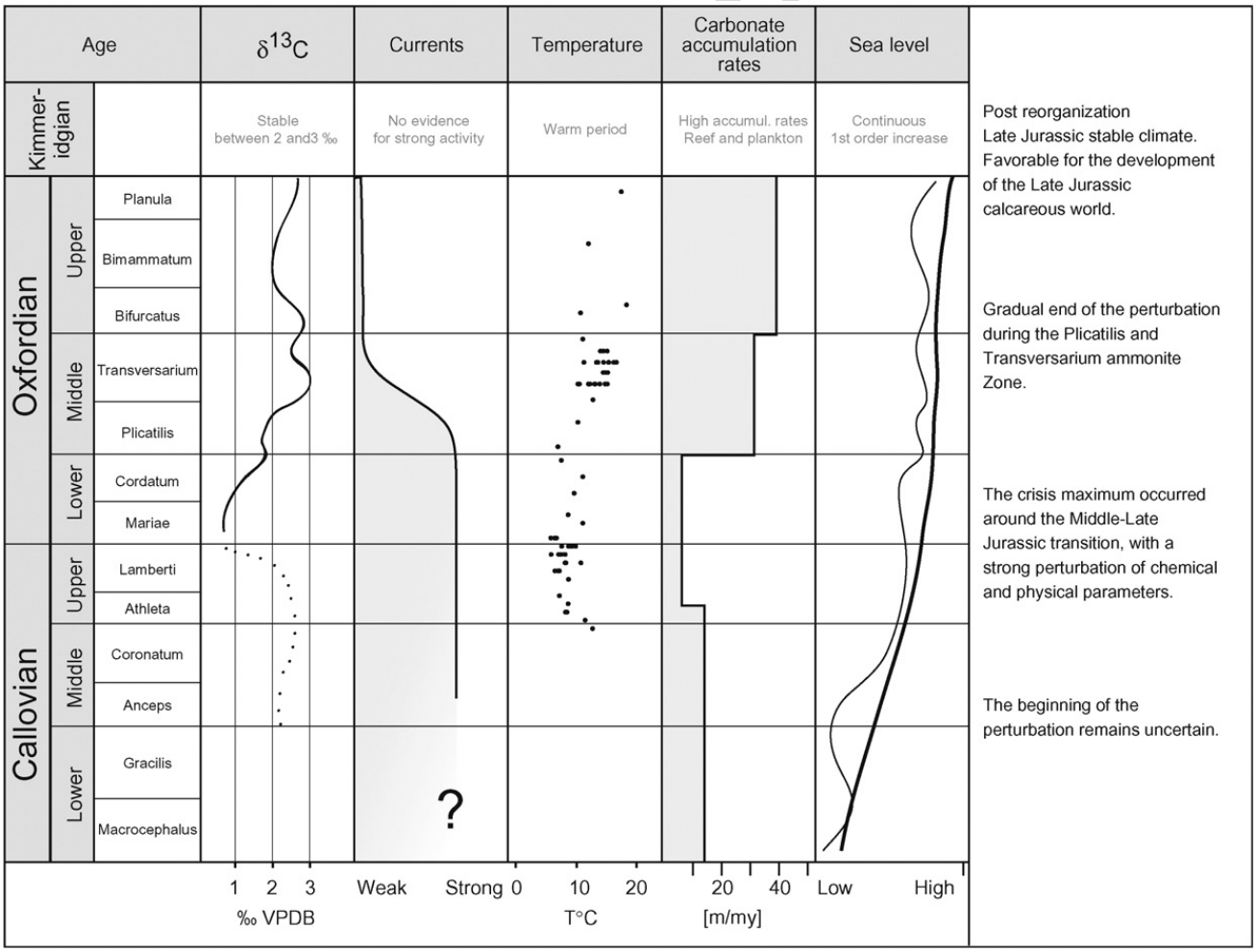

Fig. 10. Comparison of the measured C-isotopes and the currents activity with temperature, sea-level variations and carbonate accumulation rates. $\delta^{13}C$ (dotted line) and carbonate accumulation rates after Dromart et al. (2003a). Temperatures compiled by Dromart et al. (2003a) from data by Riboulleau et al. (1998) and Veizer et al. (1999). Sea level curve after Haq et al. (1988).

6.6. A change in tectonics and oceanography

According to sedimentary and chemical records, the Oxfordian stage represents a time of major change for the Mesozoic oceanography. We propose that the breakup of the Pangaean continent (Ziegler, 1988; Scotese, 2001; Stampfli and Borel, 2002) may have caused these changes (Dercourt et al., 1994). The seafloor spreading activity was exceptionally high during Late Callovian and Oxfordian (Corbin et al., 2000; Cogne and Humler, 2004). The strontium-isotope curve ($^{87}Sr/^{86}Sr$), which reaches its lowest values of the Mesozoic in the Oxfordian (McArthur et al., 2001), may reflect the intense mid-ocean ridge hydrothermal activity (Jones et al., 1994) and highlights this period as a turning point in ocean chemistry.

The modification of small oceanic seaways might have influenced the oceanic circulation pattern during the Oxfordian, for example in the North Sea region (Riboulleau et al., 1998; Pellenard et al., 1999; Abbink et al., 2001), the closure of the Meliata Ocean (Stampfli and Borel, 2002; Csontos and Voros, 2004), or the migration of the Bihor–Getic microplate (Csontos and Voros, 2004). However, the most important change in the ocean morphology is the deepening of the Hispanic Corridor separating Laurasia and Gondwana. The first shallow-water connection between Tethys/Atlantic and Pacific is dated as Pliensbachian–Toarcian by bivalve migration (Aberhan, 2001). Through continuous deepening of the Hispanic Corridor associated with a first order sea-level rise, a seaway that allowed significant water mass exchange between the two basins was established during the Late Jurassic (Riccardi, 1991; Winterer, 1991; Stille et al., 1996; Hallam, 2001; Hotinski and Toggweiler, 2003). Studies on reef development (Leinfelder et al., 2002) or brachiopods (Ager and Walley, 1977; Voros, 1993) confirm the establishment of a first true seaway around the Callovian–Oxfordian boundary.

Climate models reveal that the opening of a low latitude passage triggered a reorganization of ocean current pattern with a new existing east–west current system and the improvement of latitudinal heat exchange (Winterer, 1991; Hotinski and Toggweiler, 2003), which caused the warming of high-latitude surface water (Riboulleau et al., 1998; Abbink et al., 2001). The change in oceanography resulted in the reduction of moisture transport to these latitudes, and to the Late Jurassic shift to drier conditions (Abbink et al., 2001). In other words, the Middle–Late Jurassic change in oceanography corresponds to at least a partial breakdown of the previous megamonsoonal climate system (Parrish, 1993) and the onset of a circumequatorial ocean circulation, which persisted until the Cenozoic (Winterer, 1991; Moore et al., 1992; Hotinski and Toggweiler, 2003). The rifting of Laurasia from Gondwana removed the principal forcing factor of the Early Mesozoic megamonsoon, the Pangaean geography. The homogenization of the surface temperature, the establishment of a dry low latitude climate belt combined with the expansion of new epicontinental seas offered ideal conditions for the widespread carbonate deposition in Late Jurassic neritic and deep water environments.

Acknowledgements

This project was supported by the Swiss Science Foundation, grant No. 2-77549-04. We thank the Swiss National Cooperative for the Storage of Radioactive Waste (NAGRA) for providing us the samples of the Weiach section. Thanks to Flavio Anselmetti for providing information and samples from the Marion Plateau. Finally, we would like to thank the two anonymous reviewers for their constructive comments on the original manuscript.

References

Abbink, O., Targarona, J., Brinkhuis, H., Visscher, H., 2001. Late Jurassic to earliest Cretaceous palaeoclimatic evolution of the southern North Sea. Glob. Planet. Change 30 (3–4), 231–256.

Aberhan, M., 2001. Bivalve palaeobiogeography and the Hispanic Corridor; time of opening and effectiveness of a proto-Atlantic seaway. Palaeogeogr. Palaeoclimatol. Palaeoecol. 165 (3–4), 375–394.

Ager, D.V., Walley, C.D., 1977. Mesozoic brachiopod migrations and the opening of the North Atlantic. Palaeogeogr. Palaeoclimatol. Palaeoecol. 21 (2), 85–99.

Aghib, F.S., Bernoulli, D., Weissert, H., 1991. Hardground formation in the Bannock Basin, eastern Mediterranean. In: Cita Maria, B., de Lange Gert, J., Olausson, E. (Eds.), Anoxic basins and sapropel deposition in the eastern Mediterranean; past and present. Elsevier, Amsterdam, Netherlands, pp. 103–113.

Allenbach, R.P., 2001. Synsedimentary tectonics in an epicontinental sea: A new interpretation of the Oxfordian basins of northern Switzerland. Eclogae Geol. Helv. 94, 265–287.

Bartolini, A., Baumgartner, P.O., Hunziker, J.C., 1996. Middle and Late Jurassic carbon stable-isotope stratigraphy and radiolarite sedimentation of the Umbria–marche Basin (Central Italy). Eclogae Geol. Helv. 89, 831–879.

Baumgartner, P.O., 1987. Age and genesis of Tethyan Jurassic radiolarites. Eclogae Geol. Helv. 80 (3), 831–879.

Besairie, H., Collignon, M., 1971. Géologie de Madagascar. I. Les Terrains sédimentaires. Ann. Géol. Madag. 35.

Bombardiere, L., Gorin, G.E., 2000. Stratigraphical and lateral distribution of sedimentary organic matter in Upper Jurassic carbonates of SE France. Sediment. Geol. 132 (3–4), 177–203.

Burkhalter, R.M., 1995. Ooidal ironstones and ferruginous microbialites; origin and relation to sequence stratigraphy (Aalenian and Bajocian, Swiss Jura Mountains). Sedimentology 42 (1), 57–74.

Cecca, F., Savary, B., Bartolini, A., Remane, J., Cordey, F., 2001. The Middle Jurassic–Lower Cretaceous Rosso Ammonitico succession of Monte Inici (Trapanese Domain, western Sicily); sedimentology, biostratigraphy and isotope stratigraphy. Bull. Soc. Geol. Fr. 172 (5), 647–659.

Cecca, F., Martin Garin, B., Marchand, D., Lathuiliere, B., Bartolini, A., 2005. Paleoclimatic control of biogeographic and sedimentary events in Tethyan and peri-Tethyan areas during the Oxfordian (Late Jurassic). Palaeogeogr. Palaeoclimatol. Palaeoecol. 222 (1–2), 10–32.

Cogne, J.-P., Humler, E., 2004. Temporal variation of oceanic spreading and crustal production rates during the last 180 My. Earth Planet. Sci. Lett. 227, 427–439.

Collin, P.Y., Loreau, J.P., Courville, P., 2005. Depositional environments and iron ooid formation in condensed sections (Callovian–Oxfordian, south-eastern Paris basin, France). Sedimentology 52 (5), 969–987.

Corbin, J.C., Person, A., Iatzoura, A., Ferre, B., Renard, M., 2000. Manganese in pelagic carbonates; indication of major tectonic events during the geodynamic evolution of a passive continental margin (the Jurassic European margin of the Tethys–Ligurian Sea). Palaeogeogr. Palaeoclimatol. Palaeoecol. 156 (1–2), 123–138.

Cordey, F., Boughdiri, M., Sallouhi, H., 2005. First direct age determination from the Jurassic radiolarian-bearing siliceous series (Jédidi Formation) of northwestern Tunisia. C.R. Geosci. 337 (8), 777–785.

Cottereau, N., Lautenschlager, M., 1994. Tethyan oceanic circulations during the Latest Jurassic; a GCM simulation. C.R. Acad. Sci., Ser II 318 (3), 389–396.

Csontos, L., Voros, A., 2004. Mesozoic plate tectonic reconstruction of the Carpathian region. Palaeogeogr. Palaeoclimatol. Palaeoecol. 210 (1), 1–56.

Dercourt, J., Fourcade, E., Cecca, F., Azema, J., Enay, R., Bassoullet, J.P. and Cottereau, N., 1994. Palaeoenvironment of the Jurassic system in the Western and Central Tethys (Toarcian, Callovian, Kimmeridgian, Tithonian); an overview. In: Geobios (Ed.), 3eme Symposium international de stratigraphie du Jurassique. Memoire Special 17, pp. 625–644.

Dollfus, S., 1961. Über das Alter des Blegi–Ooliths in der Glärnisch–Gruppe. Mitt. Geol. Inst. Eidgenoss. Tech. Hochsch. Univ. Zur. 302.

Dromart, G., 1992. Jurassic deep-water microbial biostromes as flooding markers in carbonate sequence stratigraphy. In: Cotillon, P. (Ed.), Mesozoic eustacy record on western Tethyan margins. Elsevier, Amsterdam, Netherlands, pp. 219–228.

Dromart, G., Garcia, J.P., Gaumet, F., Picard, S., Rousseau, M., Atrops, F., Lecuyer, C., Sheppard, S.M.F., 2003a. Perturbation of the carbon cycle at the Middle/Late Jurassic transition; geological and geochemical evidence. Am. J. Sci. 303 (8), 667–707.

Dromart, G., Garcia, J.P., Picard, S., Atrops, F., Lécuyer, C., Sheppard, S.M.F., 2003b. Ice age at the Middle–Late Jurassic transition? Earth Planet. Sci. Lett. 213, 205–220.

Enay, R., 1980. Paleobiogeographie et Ammonites jurassiques; "rythmes fauniques" et variations du niveau marin; voies d'echanges, migrations et domaines biogeographiques. Livre jubilaire du cent cinquantenaire 1830–1980, pp. 261–281.

Fatmi, A.N., 1972. Stratigraphy of the Jurassic and lower Cretaceous rocks and Jurassic ammonites from northern areas of West Pakistan. Bull. Br. Mus., Nat. Hist., Geol. Ser. 20 (7), 301–380.

Fluegel, E., 2004. Microfacies of carbonate rocks; analysis, interpretation and application. Springer, Berlin.

Fuersich, F.T., 1979. Genesis, environments, and ecology of Jurassic hardgrounds. Neues Jahrb. Geol. Palaeontol. 158 (1), 1–63.

Fuersich, F.T., Oschmann, W., Singh, I.B., Jaitly, A.K., 1992. Hardgrounds, reworked concretion levels and condensed horizons in the Jurassic of western India; their significance for basin analysis. J. Geol. Soc. (Lond.) 149 (3), 313–331.

Furrer, U., 1979. Stratigraphie des Doggers der oestlichen Prealpes medianes (Stockhorn–Gebiet zwischen Blumenstein und Boltigen, Kt. Bern). Eclogae Geol. Helv. 72 (3), 623–672.

Gaillard, C., Atrops, F., Marchand, D., Hanzo, M., Lathuiliere, B., Bodeur, Y., Ruget, C., Nicoullin, J.P., Werner, W., 1996. Description stratigraphique préliminaire des faisceaux alternants de l'Oxfordien moyen dans le bassin dauphinois (Sud–Est de la France). Géol. Fr. 1, 17–24.

Gaillard, C., Emmanuel, L., Hanzo, M., Lathuiliere, B., Atrops, F., Bodeur, Y., Bouhamdi, A., Marchand, D., Enay, R., Ruget, C., Werner, W., 2004. Une séquence disséquée du bassin à la plateforme: l'épisode carbonaté de l'Oxfordien moyen dans le Sud–Est de la France. Bull. Soc. Geol. Fr. 175, 107–119.

Garrison, R.E., Fischer, A.G., 1969. Deep-water limestones and radiolarites of the Alpine Jurassic. In: Friedman, G.M. (Ed.), Depositional environments in carbonate rocks; a symposium. Soc. Econ. Paleonto. Mineralo., pp. 20–56.

Gehring, A.U., 1986. Untersuchungen zur Bildung von Eisenoolithen. Ph. D. thesis, ETH Zurich.

Gradstein, F.M., Ogg, J.G., Smith, A.G., Agterberg, F.P., Bleeker, W., Cooper, R.A., Davydov, V., Gibbard, P., Hinnov, L., House, M.R., Lourens, L., Luterbacher, H.P., McArthur, J., Melchin, M.J., Robb, L.J., Shergold, J., Villeneuve, M., Wardlaw, B.R., Ali, J., Brinkhuis, H., Hilgen, F.J., Hooker, J., Howarth, R.J., Knoll, A.H., Laskar, J., Monechi, S., Plumb, K.A., Powell, J., Raffi, I., Roehl, U., Sanfilippo, A., Schmitz, B., Shackleton, N.J., Shields, G.A., Strauss, H., van, D.J., van, K.T., Veizer, J., Wilson, D., 2004. A geological time scale 2004. Geological Survey of Canada, Ottawa, Canada.

Gygi, R.A., 1981. Oolitic iron formations; marine or not marine? Eclogae Geol. Helv. 74 (1), 233–254.

Gygi, R.A., 1986. Eustatic sea level changes of the Oxfordian (Late Jurassic) and their effect documented in sediments and fossil assemblages of an epicontinental sea. Eclogae Geol. Helv. 79 (2), 455–491.

Gygi, R.A., 2000. Integrated stratigraphy of the Oxfordian and Kimmeridgian (Late Jurassic) in northern Switzerland and adjacent southern Germany. Birkhauser Verlag, Basel, Switzerland.

Gygi, R.A., Marchand, D., 1982. Les faunes de Cardioceratinae (Ammonoidea) du Callovien terminal et de l'Oxfordien inferieur et moyen (Jurassique) de la Suisse septentrionale; stratigraphie, paleoecologie, taxonomie preliminaire. Geobios 15 (4), 517–571.

Gygi, R.A., Persoz, F., 1986. Mineralostratigraphy, litho- and biostratigraphy combined in correlation of the Oxfordian (Late Jurassic) formations of the Swiss Jura Range. Eclogae Geol. Helv. 79 (2), 385–454.

Hallam, A., 1985. A review of Mesozoic climate. J. Geol. Soc. (Lond.) 142 (3), 433–445.

Hallam, A., 2001. A review of the broad pattern of Jurassic sea-level changes and their possible causes in the light of current knowledge. Palaeogeogr. Palaeoclimatol. Palaeoecol. 167 (1–2), 23–37.

Haq, B.U., Hardenbol, J., Vail, P.R., 1988. Mesozoic and Cenozoic chronostratigraphy and cycles of sea-level change. In: Wilgus Cheryl, K., Hastings Bruce, S., Ross Charles, A., Posamentier Henry, W., Van Wagoner, J., Kendall Christopher, G.S.C. (Eds.), Sea-level changes; an integrated approach. SEPM (Society for Sedimentary Geology), Tulsa OK, United States, pp. 72–108.

Hautevelle, Y., 2005. Géochimie organique des série argilo-carbonatées du Callovo–Oxfordien de l'Est du bassin de Paris et

d'Angleterre. Variabilités et implications paléoenvironnementales. Ph. D. Thesis, Université Henri Poincaré.

Heck, P.R., Frank, M., Anselmetti Flavio, S. and Kubik, P.W., in prep. Origin and age of submarine ferromanganese hardgrounds from the Marion Plateau, offshore NE Australia.

Homewood, P., Winkler, W., 1977. Les calcaires détritiques et noduleux du Malm des Médianes Platiques dans les Préalpes fribourgeoises. Bull. Soc. Fribg. Sci. Nat. 66 (2), 116–140.

Hotinski, R.M., Toggweiler, J.R., 2003. Impact of a Tethyan circumglobal passage on ocean heat transport and "equable" climates. Paleoceanography 18 (1), 7.

Isern, A.R., Anselmetti, F.S., Blum, P., Andresen, N., Birke, T.K., Bracco, G.G.L., Burns, S.J., Conesa, G.A.R., Delius, H., Dugan, B., Eberli, G.P., Ehrenberg, S., Fuller, M.D., Muller, P.H., Hine, A.C., Howell, M.W., John, C.M., Karner, G.D., Kindler, P.F., Olson, B.E., Sasaki, K., Stewart, D., Wei, W., White, T.S., Wood, J.L., Yamada, T., 2001. Sites 1196 and 1199. Correlation of deep sea sediments and forereef carbonates in the Red Sea; an important clue for basin analysis. The Marion plateau carbonates (NE Australia); a platform-slope-shelf edifice shaped by sea level change and ocean currents. In: Isern Alexandra, R., Anselmetti Flavio, S., Blum, P., Andresen, N., Birke Tesfaye, K., Bracco Gartner Guido, L., Burns Stephen, J., Conesa Gilles, A.R., Delius, H., Dugan, B., Eberli Gregor, P., Ehrenberg, S., Fuller Michael, D., Muller Pamela, H., Hine Albert, C., Howell Michael, W., John Cedric, M., Karner Garry, D., Kindler Pascal, F., Olson Brooke, E., Sasaki, K., Stewart, D., Wei, W., White Timothy, S., Wood Jason, L., Yamada, T., May Krista, L., Nevill Heather, M., Cagle Lori, J., Anonymous (Eds.), Proceedings of the Ocean Drilling Program; initial reports; constraining Miocene sea level change from carbonate platform evolution, Marion Plateau, Northeast Australia; covering Leg 194 of the cruises of the drilling vessel JOIDES Resolution, Townsville, Australia, to Apra Harbor, Guam, sites, vol. 1192–1199, pp. 255–267. 3 January–2 March.

James, N.P., Bone, Y., Collins, L.B., Kyser, T.K., 2001. Surficial sediments of the Great Australian Bight; facies dynamics and oceanography on a vast cool-water carbonate shelf. J. Sediment. Res. 71 (4), 549–567.

Jenkyns, H.C., 1996. Relative sea-level change and carbon isotopes; data from the Upper Jurassic (Oxfordian) of central and southern Europe. Terra Nova 8 (1), 75–85.

Jones, C.E., Jenkyns, H.C., Coe, A.L., Hesselbo, S.P., 1994. Strontium isotopic variations in Jurassic and Cretaceous seawater. Geochim. Cosmochim. Acta 58 (14), 3061–3074.

Kugler, C., 1987. Die Wildegg Formation im Ostjura und die Schilt-Formation um oestlichen Helvetikum; ein Vergleich. Ph. D. thesis, ETH Zurich.

Lantzsch, H., Roth, S., Reijmer, J.J.G. and Egenhoff, S., 2005. Sea-level related resedimentation processes on the northern slope of the Little Bahama Bank. In: 2005, E.G.U. (Ed.), Geophysical Research Abstracts.

Legarreta, L., 1991. Evolution of a Callovian–Oxfordian carbonate margin in the Neuquen Basin of west-central Argentina; facies, architecture, depositional sequences and global sea-level changes. In: Biddle, K.T., Schlager, W. (Eds.), The record of sea-level fluctuations. Elsevier, Amsterdam, Netherlands, pp. 209–240.

Leinfelder, R.R., Schmid, D.U., Nose, M., Werner, W., 2002. Jurassic reef patterns; the expression of a changing globe. In: Kiessling, W., Fluegel, E., Golonka, J. (Eds.), Phanerozoic reef patterns. Soc. Sediment. Geol. SEPM, Tulsa, US.

Louis-Schmid, B., 2006. Feedback mechanisms between carbon cycling, climate and oceanography: a combined geochemical, sedimentological and modeling approach. Ph. D. thesis, ETH Zurich.

Louis-Schmid, B., Rais, P., Bernasconi, S.M., Pellenard, P., Collin, P.Y., Weissert, H., 2007. Detailed record of the mid-Oxfordian (Late Jurassic) positive carbon-isotope excursion in two hemipelagic sections (France and Switzerland): a plate tectonic trigger? Palaeogeogr. Palaeoclimatol. Palaeoecol. 248 (3–4), 459–472.

Lécuyer, C., Picard, S., Garcia, J.P., Sheppard, S.M.F., Grandjean, P., Dromart, G., 2003. Thermal evolution of Tethyan surface waters during the Middle–Late Jurassic: Evidence from ∂18O values of marine fish teeth. Paleoceanography 18 (3), 1076.

Marshall, J.D., Ashton, M., 1980. Isotopic and trace element evidence for submarine lithification of hardgrounds in the Jurassic of eastern England. Sedimentology 27 (3), 271–289.

Matter, A., Peters, T., Blasi, H.R., Meyer, J., Ischi, H., Meyer, C., 1988. Sondierbohrung Weiach; Geologie. Landeshydrologie und-geologie. Bundesamt fuer Umweltschutz, Bern, Switzerland.

McArthur, J.M., Howarth, R.J., Bailey, T.R., 2001. Strontium isotope stratigraphy; LOWESS Version 3; best fit to the marine Sr-isotope curve for 0–509 Ma and accompanying look-up table for deriving numerical age. J. Geol. 109 (2), 155–170.

Mettraux, M., Weissert, H., Homewood, P., 1989. An oxygen-minimum palaeoceanographic signal from early Toarcian cavity fills. J. Geol. Soc. (Lond.) 146 (2), 333–344.

Moore, G.T., Hayashida, D.N., Ross, C.A., Jacobson, S.R., 1992. Paleoclimate of the Kimmeridgian/ Tithonian (Late Jurassic) world; I, Results using a general circulation model. Palaeogeogr. Palaeoclimatol. Palaeoecol. 93 (1–2), 113–150.

Mullins, H.T., Neumann, A.C., Wilber, R.J., Boardman, M.R., 1980. Nodular carbonate sediment on Bahamian slopes; possible precursors to nodular limestones. J. Sediment. Petrol. 50 (1), 117–131.

Mutti, M., Bernoulli, D., 2003. Early marine lithification and hardground development on a Miocene ramp (Maiella, Italy); key surfaces to track changes in trophic resources in nontropical carbonate settings. J. Sediment. Res. 73 (2), 296–308.

Norris, M.S., Hallam, A., 1995. Facies variations across the Middle–Upper Jurassic boundary in Western Europe and the relationship to sea-level changes. Palaeogeogr. Palaeoclimatol. Palaeoecol. 116 (3–4), 189–245.

Padden, M., Weissert, H., de Rafelis, M., 2001. Evidence for Late Jurassic release of methane from gas hydrate. Geology 29 (3), 223–226.

Padden, M., Weissert, H., Funk, H., Schneider, S., Gansner, C., 2002. Late Jurassic lithological evolution and carbon-isotope stratigraphy of the western Tethys. Eclogae Geol. Helv. 95, 333–346.

Parrish, J.T., 1993. Climate of the supercontinent Pangea. J. Geol. 101 (2), 215–233.

Pellenard, P., 2003. Message terrigène et influences volcaniques au Callovien–Oxfordien dans les bassins de Paris et du sud-est de la France.

Pellenard, P., Deconinck, J.F., Marchand, D., Thierry, J., Fortwengler, D., Vigneron, G., 1999. Controle geodynamique de la sedimentation argileuse du Callovien–Oxfordien moyen dans l'est du bassin de Paris; influence eustatique et volcanique. C.R. Acad. Sci., Ser II 328 (12), 807–813.

Riboulleau, A., Baudin, F., Daux, V., Hantzpergue, P., Renard, M., Zakharov, V., 1998. Evolution de la paleotemperature des eaux de la plate-forme russe au cours du Jurassique superieur. C.R. Acad. Sci., Ser II 326 (4), 239–246.

Riccardi, A.C., 1991. Jurassic and Cretaceous marine connections between the Southeast Pacific and Tethys. In: Channell James, E.T., Winterer Edward, L., Jansa Lubomir, F. (Eds.), Palaeogeography and paleoceanography of Tethys, pp. 155–189.

Rioult, M., Dugue, O., Jan, D.C.R., Ponsot, C., Fily, G., Moron, J.M., Vail, P.R., 1991. Outcrop sequence stratigraphy of the Anglo-Paris

Basin, Middle to Upper Jurassic (Normandy, Maine, Dorset). Bull. Cent. Rech. Explor. Prod. Elf-Aquitaine 15 (1), 101–194.

Sandy, M.R., 1991. Aspects of Middle–Late Jurassic–Cretaceous Tethyan brachiopod biogeography in relation to tectonic and paleoceanographic developments. In: Channell James, E.T., Winterer Edward, L., Jansa Lubomir, F. (Eds.), Palaeogeography and paleoceanography of Tethys, pp. 137–154.

Schlager, W., 1974. Preservation of cephalopod skeletons and carbonate dissolution on ancient Tethyan sea floors. In: Hsu, K.J., Jenkyns, H.C. (Eds.), Pelagic sediments: on land and under sea. IAS Spec. Publ.

Schlager, W., 1989. Drowning unconformities on carbonate platforms. In: Crevello Paul, D., Wilson James, J., Sarg, J.F., Read, J.F. (Eds.), Controls on carbonate platform and basin development, pp. 15–25.

Scotese, C.R., 2001. Atlas of Earth History. PALEOMAP Project, Arlington, Texas.

Smith, A.G., Smith, D.G., Funnell, B.M., 1994. Atlas of Mesozoic and Cenozoic Coastlines. Cambrige University Press.

Stampfli, G.M., Borel, G.D., 2002. A plate tectonic model for the Paleozoic and Mesozoic constrained by dynamic plate boundaries and restored synthetic oceanic isochrons. Earth Planet. Sci. Lett. 196 (1–2), 17–33.

Stille, P., Steinmann, M., Riggs, S.R., 1996. Nd isotope evidence for the evolution of the paleocurrents in the Atlantic and Tethys oceans during the past 180 Ma. Earth Planet. Sci. Lett. 144 (1–2), 9–19.

Thierry, J., Abbate, E., Alekseev, A.S., Ait, O.R., Ait, S.H., Bouaziz, S., Canerot, J., Georgiev, G., Guiraud, R., Hirsch, F., Ivanik, M., Le, M.J., Le, N.Y.M., Medina, F., Mouty, M., Nazarevich, B., Nikishin, A.M., Page, K., Panov, D.L., Pique, A., Poisson, A., Sandulescu, M., Sapunov, I.G., Seghedi, A., Soussi, M., Tchoumatchenko, P.V., Vaslet, D., Vishnevskaya, V., Volozh, Y.A., Voznezenski, A., Walley, C.D., Wong, T.E., Ziegler, M., Barrier, E., Bergerat, F., Bracene, R., Brunet, M.F., Cadet, J.P., Guezou, J.C., Jabaloy, A., Lepvrier, C., Rimmele, G., de, W.P., Baudin, F., Belaid, A., Bonneau, M., Coutelle, A., Fekirine, B., Guillocheau, F., Hantzpergue, M., Julien, M., Kokel, F., Lamarche, J., Mami, L., Mansy, J.L., Mascle, G., Pascal, C., Robin, C., Stephenson, R., Sihamdi, N., Vera, J.A., Vuks, V.J., 2000a. Early Kimmeridgian (146–144 Ma). In: Dercourt, J., Gaetani, M., Vrielynck, B., Barrier, E., Biju Duval, B., Brunet, M.F., Cadet, J.P., Crasquin, S., Sandulescu, M. (Eds.), Peri-Tethys atlas; palaeogeographical maps; explanatory notes.

Thierry, J., Barrier, E., Abbate, E., Ait, O.R., Ait, S.H., Bouaziz, S., Canerot, J., Elmi, S., Georgiev, G., Guiraud, R., Hirsch, F., Ivanik, M., Le, M.J., Le, N.Y.M., Medina, F., Mouty, M., Nazarevitch, V., Nikishin, A.M., Page, K., Panov, D.L., Pique, A., Poisson, A., Sandulescu, M., Sapunov, I.G., Seghedi, A., Soussi, M., Tarkowski, R.A., Tchoumatchenko, P.V., Vaslet, D., Vishnevskaya, V., Volozh, Y.A., Voznezenski, A., Walley, C.D., Wong, T.E., Ziegler, M., Ait, B.L., Bergerat, F., Bracene, R., Brunet, M.F., Cadet, J.P., Guezou, J.C., Jabaloy, A., Lepvrier, C., Rimmele, G., de, W.P., Belaid, A., Bonneau, M., Coutelle, A., Fekirine, B., Guillocheau, F., Julien, M., Kokel, F., Lamarche, J., Mami, L., Mansy, J.L., Mascle, G., Meister, C., Pascal, C., Robin, C., Sihamdi, N., Stephenson, R., Vera, J.A., Vuks, V.J., 2000b. Middle Callovian (157–155 Ma). In: Dercourt, J., Gaetani, M., Vrielynck, B., Barrier, E., Biju Duval, B., Brunet, M.F., Cadet, J.P., Crasquin, S., Sandulescu, M. (Eds.), Peri-Tethys atlas; palaeogeographical maps; explanatory notes.

Tribovillard, N.P., 1988. Geochimie organique et minerale dans les Terres Noires calloviennes et oxfordiennes du bassin dauphinois (France SE); Mise en evidence de cycles climatiques. Bull. Soc. Geol. Fr., Huitieme Serie 4 (1), 141–150.

Veizer, J., Ala, D., Azmy, K., Bruckschen, P., Buhl, D., Bruhn, F., Carden, G.A.F., Diener, A., Ebneth, S., Godderis, Y., Jasper, T., Korte, C., Pawellek, F., Podlaha, O.G., Strauss, H., 1999. 87Sr/86Sr, ∂13C and ∂18O evolution of Phanerozoic seawater. In: Veizer, J. (Ed.), Earth system evolution; geochemical perspective. Elsevier, Amsterdam, Netherlands, pp. 59–88.

Voros, A., 1993. Jurassic microplate movements and brachiopod migrations in the western part of the Tethys. In: Mancenido, M.O. (Ed.), Brachiopod and molluscan biogeography, palaeoecology and stratigraphy; a tribute to Derek Ager. Elsevier, Amsterdam, Netherlands, pp. 125–145.

Weissert, H., Mohr, H., 1996. Late Jurassic climate and its impact on carbon cycling. Palaeogeogr. Palaeoclimatol. Palaeoecol. 122 (1–4), 27–43.

Wierzbowski, H., 2002. Detailed oxygen and carbon isotope stratigraphy of the Oxfordian in central Poland. Int. J. Earth Sci. 91 (2), 304–314.

Wierzbowski, H., 2004. Carbon and oxygen isotope composition of Oxfordian–early Kimmeridgian belemnite rostra; palaeoenvironmental implications for Late Jurassic seas. Palaeogeogr. Palaeoclimatol. Palaeoecol. 203 (1–2), 153–168.

Winkler, W., 1977. Zur Geologie zwischen Gantisch und Muscherenschlund (Préalpes médianes plastiques, Préalpes externes). Diploma thesis, Univ. Freiburg.

Winterer, E.L., 1991. The Tethyan Pacific during Late Jurassic and Cretaceous times. In: Channell James, E.T., Winterer Edward, L., Jansa Lubomir, F. (Eds.), Palaeogeography and paleoceanography of Tethys. Elsevier, Amsterdam, Netherlands, pp. 253–265.

Ziegler, P.A., 1988. Evolution of the Arctic–North–Atlantic and the western Tethys. American Association of Petroleum Geologists, Tulsa, OK, United States.